JAERI-M
83-127

NEANDC (J)-92/U
INDC (JAP)-79/L

# THEORETICAL CALCULATION OF DECAY DATA OF SHORT-LIVED NUCLIDES FOR JNDC FP DECAY DATA FILE

August 1983

T. Yoshida*

日 本 原 子 力 研 究 所
Japan Atomic Energy Research Institute

JAERI-Mレポートは，日本原子力研究所が不定期に公刊している研究報告書です。
入手の問合わせは，日本原子力研究所技術情報部情報資料課（〒319-11茨城県那珂郡東海村）あて，お申しこしください。なお，このほかに財団法人原子力弘済会資料センター（〒319-11 茨城県那珂郡東海村日本原子力研究所内）で複写による実費頒布をおこなっております。

JAERI-M reports are issued irregularly.
Inquiries about availability of the reports should be addressed to Information Section, Division of Technical Information, Japan Atomic Energy Research Institute, Tokai-mura, Naka-gun, Ibaraki-ken 319-11, Japan.



編集兼発行　日本原子力研究所
印　　刷　いばらき印刷㈱

# Theoretical Calculation of Decay Data of Short-Lived Nuclides for JNDC FP Decay Data File[1)]

T. Yoshida*

Japanese Nuclear Data Committee,
Tokai Research Establishment, JAERI

(Received July 15, 1983)

It is one of unique features of the JNDC FP Decay Data File that theoretical values of $\overline{E}_\beta$ and $\overline{E}_\gamma$, average beta- and gamma-ray energies, are fully adopted for short-lived nuclides. Here, details of the theoretical estimation method of $\overline{E}_\beta$ and $\overline{E}_\gamma$ based on 'gross theory' of beta-decay are described and the numerical tables of the estimated decay data for short-lived nuclides are presented. Further, discussion is made for justification of adoption of the theoretical values instead of values derived from decay schemes from the viewpoint of the energy profile of the beta-strength function.

Keywords : Fission Product, Beta Decay, Beta Ray, Gamma Ray, Short-Lived, Gross Theory, Decay Scheme, Strength Function

1) The work was performed in the evaluation work of the Working Group of Decay Heat, Japanese Nuclear Data Committee.

*) NAIG Nuclear Research Laboratory, Nippon Atomic Industry Group Co., Ltd.

JAERI－M 83－127

# JNDC FP 崩壊データファイルのための短寿命核崩壊データの理論計算†

日本原子力研究所東海研究所シグマ研究委員会
吉田　　正*

（1983年7月15日受理）

Q値の大きな短寿命核種に対して，放出ベータ線・ガンマ線の平均エネルギー $\overline{E}_\beta$，$\overline{E}_\gamma$ の理論計算値を全面的に採用したことは，JNDC FP Decay Data File の大きな特徴である。本報告では，まずベータ崩壊の大局的理論に基づく $\overline{E}_\beta$，$\overline{E}_\gamma$ の理論的推定法を詳細に説明し，この方法で得られた短寿命核の崩壊データの数値表を示す。更に，測定に基づく崩壊スキームから計算される $\overline{E}_\beta$，$\overline{E}_\gamma$ 値のかわりに，理論値を採用したことについて，ベータ強度関数のエネルギー依存性の検討から，その正当性を明らかにする。

† ）本報告書は，シグマ研究委員会・核構造データ専門部会・崩壊熱評価ワーキング・グループの作業の一環として行われた仕事をまとめたものである。

＊）日本原子力事業株式会社，総合研究所

CONTENTS

1. Introduction ........................................ 1
2. Decay Data of Short-Lived FPs and their Theoretical Estimation ........................................ 2
3. Data for $\overline{E}_\beta$, $\overline{E}_\gamma$ and $t_{1/2}$ adopted in the JNDC File ........... 11
4. Problems in Deriving $\overline{E}_\beta$ and $\overline{E}_\gamma$ from Decay Schemes ........... 14
5. Concluding Remarks ........................................ 18
Acknowledgment ........................................ 19

目　　次

1. 序　論 ........................................ 1
2. 短寿命 FP の崩壊スキームとその理論的推定 ........................................ 2
3. JNDC ファイルで採用した $\overline{E}_\beta$, $\overline{E}_\gamma$ 及び $t_{1/2}$ データ ........................................ 11
4. 崩壊スキームから $\overline{E}_\beta$, $\overline{E}_\gamma$ を算出する際の問題点 ........................................ 14
5. まとめ ........................................ 18
謝　辞 ........................................ 19

## 1. Introduction

The origin of the fission product decay heat is the beta- and gamma-ray energies released from unstable fission products undergoing beta-decay. The most powerful and widely used tool to evaluate the size of this energy release is the summation calculation method, which is based on summing up of the contributions from all the unstable nuclides produced by fission events. In order to calculate the contribution from each nuclide, it is necessary to know the fission yield, the decay constant (or half-life), the branching ratios, and the average beta- and gamma-ray energies ($\overline{E}_\beta$, $\overline{E}_\gamma$) per one decay event. These data are physical constants inherent to each fission product (hereafter FP), and usually a set of these data for all the important FP nuclides are stored in a peripheral memory to be read by a computer code for use in summation calculations. This kind of data set is called a FP decay data file (or library) for summation calculations. Today not a few sets of FP decay data file are open to the users who are interested in decay heat calculations.[1)-5)]

In the 1970's, requirement for the high prediction accuracy of the decay heat at short cooling-times was stressed from the nuclear safety field, and it stimulated experimental and theoretical studies of the FP decay heat around the world. It was one of responses to this requirement that the Japanese Nuclear Data Committee (JNDC) started to compile a new FP decay data file in the middle of the 1970's. This file, completed in 1981 as 'JNDC FP Decay Data File'[6)], was aimed at improvement of the prediction accuracy of the FP decay heat at short cooling-times. The most serious obstacle to this goal was the fact that the decay data were scarce, or inaccurate even if available, for short-lived FPs which are the dominant contributors to the decay heat at short cooling-time. According to a study by Schmittroth et al.[7)], the uncertainty in the $\overline{E}_\beta$ and $\overline{E}_\gamma$ data is responsible for the largest portion of the total error in the calculated decay heat. In order to improve the reliability of the decay data for the 'data-unknown' FPs, the present author proposed a theoretical estimation method of $t_{1/2}$, $\overline{E}_\beta$ and $\overline{E}_\gamma$[8)] on the basis of a 'gross theory'[9),10)] of beta-decay. With the same intention several authors presented estimation method of $\overline{E}_\beta$ and $\overline{E}_\gamma$ from different approaches.[11),12)] A 'microscopic theory'[13)] of beta-decay might be an alternative theoretical basis capable of calculating $\overline{E}_\beta$ and $\overline{E}_\gamma$ for a wide range of nuclides.

The former part of the present report is devoted to a detailed description of the way in which the present author's method is applied to the estimation of $t_{1/2}$, $\overline{E}_\beta$ and $\overline{E}_\gamma$ data to be contained in the JNDC FP Decay Data File. In chapter 2 we review the gross theory of beta-decay and describe the way in which the theory is applied to estimate the unknown parameters relevant to decay heat calculations. As is described in chapter 3, the adoption of the theoretical data drastically improved the consistency between calculated and measured decay heat curves at short cooling-times. The physical interpretation of this improvement is tried in chapter 4.

## 2. Decay Data of Short-Lived FPs and their Theoretical Estimation

### 2.1 Average energies of beta- and gamma-rays emitted per one decay

Before dealing with the theoretical estimation method we review the calculation method of $\overline{E}_\beta$ and $\overline{E}_\gamma$ for data-known nuclides. Figure 1 displays a typical decay scheme of a short-lived nuclide with a relatively large $Q_\beta$-value. Beta-decay of the parent nucleus (Z,N) populates not only the ground state but also many excited levels having energy $\varepsilon_i$ with branching ratio $a_i$. At the first stage a beta-ray and an anti-neutrino are emitted and then the populated excited level is de-excited by emitting gamma-rays usually through a cascade process. The average energies of these beta- and gamma-rays per one beta-decay are expressed in terms of the branching ratios $a_i$ (here $\sum_i a_i = 1$) as

$$\overline{E}_\beta = \sum_i a_i E_\beta^{(i)} \quad \cdots\cdots\cdots\cdots \quad (1)$$

$$\overline{E}_\gamma = \sum_i a_i \varepsilon_i \quad \cdots\cdots\cdots\cdots \quad (2)$$

where $E_\beta^{(i)}$ is the average beta-ray energy associated with a beta-transition to the i-th excited level. By adding this to the average anti-neutrino energy $E_\nu^{(i)}$ we get the energy difference between the ground state of the parent and the i-th excited level of the daughter, say, $E_\beta^{(i)} + E_\nu^{(i)} = Q_\beta - \varepsilon_i$. The partition of $Q_\beta - \varepsilon_i$ into $E_\beta^{(i)}$ and $E_\nu^{(i)}$ is given when the type of the beta-transition is fixed.[14] The key quantity $a_i$ essential to evaluate the right-hand sides of Eqs. (1) and (2) is given in published decay schemes, which are constructed most commonly on the basis of the beta-gamma intensity analysis.

Here we introduce the concept of the beta-strength function, which plays a quite important role in the following description of this chapter.

The former part of the present report is devoted to a detailed description of the way in which the present author's method is applied to the estimation of $t_{1/2}$, $\overline{E}_\beta$ and $\overline{E}_\gamma$ data to be contained in the JNDC FP Decay Data File. In chapter 2 we review the gross theory of beta-decay and describe the way in which the theory is applied to estimate the unknown parameters relevant to decay heat calculations. As is described in chapter 3, the adoption of the theoretical data drastically improved the consistency between calculated and measured decay heat curves at short cooling-times. The physical interpretation of this improvement is tried in chapter 4.

## 2. Decay Data of Short-Lived FPs and their Theoretical Estimation

### 2.1 Average energies of beta- and gamma-rays emitted per one decay

Before dealing with the theoretical estimation method we review the calculation method of $\overline{E}_\beta$ and $\overline{E}_\gamma$ for data-known nuclides. Figure 1 displays a typical decay scheme of a short-lived nuclide with a relatively large $Q_\beta$-value. Beta-decay of the parent nucleus (Z,N) populates not only the ground state but also many excited levels having energy $\varepsilon_i$ with branching ratio $a_i$. At the first stage a beta-ray and an anti-neutrino are emitted and then the populated excited level is de-excited by emitting gamma-rays usually through a cascade process. The average energies of these beta- and gamma-rays per one beta-decay are expressed in terms of the branching ratios $a_i$ (here $\sum_i a_i = 1$) as

$$\overline{E}_\beta = \sum_i a_i E_\beta^{(i)} \quad \ldots\ldots\ldots\ldots\ldots \quad (1)$$

$$\overline{E}_\gamma = \sum_i a_i \varepsilon_i \quad \ldots\ldots\ldots\ldots\ldots \quad (2)$$

where $E_\beta^{(i)}$ is the average beta-ray energy associated with a beta-transition to the i-th excited level. By adding this to the average anti-neutrino energy $E_\nu^{(i)}$ we get the energy difference between the ground state of the parent and the i-th excited level of the daughter, say, $E_\beta^{(i)} + E_\nu^{(i)} = Q_\beta - \varepsilon_i$. The partition of $Q_\beta - \varepsilon_i$ into $E_\beta^{(i)}$ and $E_\nu^{(i)}$ is given when the type of the beta-transition is fixed.[14] The key quantity $a_i$ essential to evaluate the right-hand sides of Eqs. (1) and (2) is given in published decay schemes, which are constructed most commonly on the basis of the beta-gamma intensity analysis.

Here we introduce the concept of the beta-strength function, which plays a quite important role in the following description of this chapter.

Let us suppose $\lambda$ is the decay constant of the parent. Then $\lambda_i = a_i \cdot \lambda$ becomes a partial decay constant associated with the beta-transition which populates the i-th excited level. In the decay of a short-lived nuclide with a high $Q_\beta$-value, the density of the final levels is high except at low excitation energy. It is, therefore, often helpful to average $\lambda_i$ in a suitable energy interval and to express it as a function of the excitation energy $\varepsilon$ of the final level. The beta-strength function $S_\beta(\varepsilon)$ is proportional to $\overline{\lambda}_i \cdot \rho/f$, where f is the integrated Fermi function[14] and $\rho$ is the level density at $\varepsilon$. The bar on $\lambda_i$ indicates that an average should be taken around $\varepsilon_i$. As f and $\rho$ are known quantities, apart from some ambiguity in $\rho$, to know $S_\beta(\varepsilon)$ is essentially equivalent to know $a_i$ as long as we are interested in the calculation of $\overline{E}_\beta$ and $\overline{E}_\gamma$. In this section we denoted the strength function as $S_\beta(\varepsilon)$. In the following sections, however, it is written as $|M(E_g)|^2$ in accordance with the convention used in the original papers of the gross theory.[9] (See Note 1 below).

## 2.2 The gross theory of beta-decay

In this section we review the gross theory which is applied to estimate $t_{1/2}$, $\overline{E}_\beta$ and $\overline{E}_\gamma$. For simplicity we restrict the description within the allowed transitions. The energy spectrum of the beta-ray emitted at a transition from the ground state of the parent having a wave function $\Psi$ to the n-th level with a wave function $\Psi_n$ is expressed as

$$\Pi_n(E)dE = \frac{mc^2}{\hbar}\frac{G^2}{2\pi^3}\left[|(\Psi_n, \Omega_F\Psi)|^2 + \frac{C_A^2}{C_V^2}|(\Psi_n, \Omega_{GT}\Psi)|^2\right]$$

$$\times F(Z+1, E)pE(E_n - E)^2 dE. \quad \ldots\ldots \quad (3)$$

Here the symbols $\Omega_F$ and $\Omega_{GT}$ represent the transition operators for the Fermi type and the Gamow-Teller type beta-transitions. The absolute value of the ratio of the axial-vector coupling constant $C_A$ to the vector coupling constant $C_V$, namely $|C_A/C_V|$, is determined experimentally to be 1.239±0.011. The dimensionless number G which appears in the factor on the top of the

---

Note 1) The energy scale is shifted by $Q_\beta$ from $\varepsilon$ to $E_g$, namely, $E_g = \varepsilon - Q_\beta$. We resume the notation $S_\beta(\varepsilon)$ in the final part of this report (Section 4.2).

right hand side of Eq. (3) has a value $(3.001\pm0.002) \times 10^{-12}$, which is reduced from the ft value for a pure Fermi-transition.[note 2] The Fermi function F(Z,N) is expressed as

$$F(Z,E) = 2(1 + \gamma)(2pR)^{2\gamma-2}\exp(\pi\nu)\frac{|\Gamma(\gamma + i\nu)|^2}{[\Gamma(2\gamma + 1)]^2} ,$$

where $\gamma = (1 - \alpha^2 Z^2)^{1/2}$, $\nu = \alpha ZE/p$, $\alpha = 1/137$ and R is the nuclear radius. Although we measure the energy and momentum of the electron in a unit of $m = c = 1.0$, we leave the factor $\hbar/mc^2$ as it is in the following expressions. In the Eq. (3) $E_n$ is the relativistic maximum electron energy emitted at a beta-transition to the n-th excited level; by use of the symbols in Fig. 1 it is equal to $Q_\beta - \varepsilon_n + 1$. The average energy of the beta- and gamma-rays, $\overline{E}_\beta^{(n)}$ and $\overline{E}_\gamma^{(n)}$, and the partial decay constant relevant to a transition to the n-th final level are expressed as

$$\overline{E}_\beta^{(n)} = \frac{1}{\lambda_n}\int_1^{E_n} (E - 1)\Pi_n(E)dE \quad \ldots\ldots\ldots\ldots \quad (4)$$

$$\overline{E}_\gamma^{(n)} = Q_\beta - E_n + 1 \quad \ldots\ldots\ldots\ldots\ldots \quad (4')$$

$$\lambda_n = \int_1^{E_n} \Pi_n(E)dE , \quad \ldots\ldots\ldots\ldots\ldots \quad (4'')$$

where $\Pi_n(E)$ is given by Eq. (3). In actual situations of the short-lived FPs, where many final levels are energetically accessible, we must sum up $\lambda_n$ over n to get the total decay constant $\lambda$.

$$\lambda = \sum_n \lambda_n$$

$$= \frac{mc^2}{\hbar}\frac{G^2}{2\pi^3}\sum_n\left[|(\Psi_n, \Omega_F\Psi)|^2 + \frac{C_A^2}{C_V^2}|(\Psi_n, \Omega_{GT}\Psi)|^2\right]$$

$$\times f(E_n) . \quad \ldots\ldots\ldots\ldots \quad (5)$$

The function $f(E_n)$ which appears in the above expression is called the integrated Fermi function and is written as

---

Note 2) The number G is related to the vector constant ($|C_V| \cong 1.405 \times 10^{-49}$ erg·cm$^3$) through an expression $C_V^2 = G^2\frac{\hbar^6}{m^4c^2}$ .

$$f(E_n) = \int_1^{E_n} F(Z + 1, E)pE(E_n - E)^2 dE \quad . \; . \; . \; . \; . \; . \; . \; . \qquad (5')$$

The starting point of the gross theory[15] of beta-decay lies in a replacement of the summation over n by an integration with the energy $E_g$ which is equal to $-(E_n - 1)$, as the variable; resultingly,

$$\lambda = \frac{mc^2}{\hbar}\frac{G^2}{2\pi^3}\int_{-Q_\beta}^{0}\left[|M_F(E_g)|^2 + 3\,\frac{C_A^{\;2}}{C_V^{\;2}}|M_{GT}(E_g)|^2\right]$$

$$\times\ f(-E_g + 1)dE_g \; . \quad . \; . \; . \; . \; . \; . \; . \; . \; . \; . \; . \; . \; . \qquad (6)$$

It is a conventional notation of the original papers of the gross theory[9] to use $E_g$ as energy variable. ($E_g$ is, in other words, the mass change in the neutral atom before and after the transition.) The symbol $|M_\omega(E_g)|^2$ ($\omega$ = F or GT) denotes the beta-strength function and is equal to the absolute square of transition matrix element $|(\Psi_n,\ \Omega_\omega\Psi)|^2$ multiplied by the level density around $E_g$. In Eq. (6) the factor of 3 of the Gamow-Teller term comes from an assumption that the parent nucleus is unpolarized.

The determination of the energy profile of the beta-strength function constitutes the essential part of the gross theory. Yamada and Takahashi[9] carried out this with the aid of the sum rules as follows.

$$\int_{-Q_\beta}^{\infty}|M_\omega(E_g)|^2 dE_g = \sum_n^{\infty}(\Psi,\ \Omega_\omega^{\dagger}\Psi_n)(\Psi_n,\ \Omega_\omega\Psi)$$

$$= (\Psi,\ \Omega_\omega^{\dagger}\Omega_\omega\Psi_n) \quad . \; . \; . \; . \; . \; . \; . \; . \; . \; . \; . \qquad (7)$$

$$\int_{-Q_\beta}^{\infty}E_g|M_\omega(E_g)|^2 dE_g = (\Psi,\ \Omega^{\dagger}[H,\ \Omega]\Psi) \quad . \; . \; . \; . \; . \; . \qquad (8)$$

$$\int_{-Q_\beta}^{\infty}E_g^{\;2}|M_\omega(E_g)|^2 dE_g = (\Psi,\ [\Omega^{\dagger},\ H][H,\ \Omega]\Psi)\ . \quad . \; . \; . \; . \qquad (9)$$

In order to refine the theory they introduced an one-particle strength function $D_\omega(E_g,\ \xi)$ by decomposing the total strength into the contributions from individual nucleons in the nucleus as

$$|M_\omega(E_g)|^2 = \int_{\xi_{min}}^{\xi_{max}} D_\omega(E_g,\ \xi)\cdot W(E_g,\ \xi)\frac{dn_1}{d\xi}\,d\xi \ , \quad . \; . \; . \; . \qquad (10)$$

where $\xi$ is the energy of the nucleon undergoing decay, $W(E_g,\ \xi)$ is a factor representing the effect of the Pauli's exclusion principle, and $\frac{dn_1}{d\xi}$ is the one particle level density of the initial state.

Here we give, as an example, the form of the one-particle strength function for the Fermi-type transition;

$$D_F(E_g, \xi) = \frac{\sigma_c{}^2 + \gamma^2}{\pi} \frac{\sigma_c{}^2}{\gamma} \frac{1}{(E_g - \Delta_c)^2 + (\sigma_c{}^2/\gamma)^2} \times \frac{1}{(E_g - \Delta_c)^2 + \gamma^2} \quad . \quad \ldots\ldots\ldots \quad (11)$$

In this case a modified-Lorentz form is assumed and the parameters $\Delta_c$ (peak position) and $\sigma_c$ (peak width) are determined with the aid of the sum rules (8) and (9) in the following way.

$$\int_{-\infty}^{\infty} E_g \cdot D_F(E_g, \xi) dE_g \equiv \Delta_c$$

$$= \left[ \frac{1.44}{(r_0/1.2)} \frac{Z}{A^{1/3}} - 0.7825 \right] \mathrm{MeV} \quad \ldots\ldots\ldots \quad (8')$$

$$\int_{-\infty}^{\infty} (E_g - \Delta_c)^2 D_F(E_g, \xi) dE_g \equiv \sigma_c{}^2$$

$$= \left[ \frac{0.157}{(r_0/1.2)} \frac{Z}{A^{1/3}} \mathrm{MeV} \right]^2 , \quad \ldots\ldots\ldots \quad (9')$$

where Z, $r_0$, and A denote the proton number of the parent, the radius of the volume occupied by one nucleon, and the mass number, respectively. The sum rule (7) has already been used to determine the normalization factor of $|M_\omega(E_g)|^2$. The expression (8') reduced from the sum rule (8) represents the sum of changes in the Coulomb energy and in the nucleon mass ($p \rightarrow n$) induced by the decay. The expression (9') gives the peak width of the strength which is brought about by the presence of the isospin impurity; in other words, if the isospin is a good quantum number, the width becomes zero. In the case of the Gamow-Teller transition, we replace $\sigma_c{}^2$ by $\sigma_c{}^2 + \sigma_N{}^2$, where $\sigma_N{}^2$ gives the increase of the width induced by incommutability of the Gamow-Teller transition operator $\Omega_{GT}$ with the spin dependent part of the nuclear force; in the present calculation $\sigma_N{}^2$ is taken to be 12 MeV.[10] In the above description we restricted the discussion within the allowed transitions. The gross theory of the forbidden transition was developed by Takahashi[17] and this is taken also into account in the present calculation. In order to apply the theory in practical problems it is essential to take into account the transitions between one-particle discrete levels. This is accomplished by using of a rather simple one-particle nuclear model. As a result the one-particle strength function is largely modified and becomes a sum of a continuum part and delta-functions representing the discrete transitions. The complete description of the procedure of obtaining the one-particle strength is too bulky to reproduce here. Refer to the original paper[18] for it. Anyway we get the total strength function by integrating the one particle strength according to the formula (1).

The gross theory expression for the decay constant $\lambda$ is given by Eq. (6). In the later part we calculate the average beta- and gamma-ray energies per one decay ($\overline{E}_\beta$, $\overline{E}_\gamma$) on the basis of the gross theory. A close parallel procedure leads to the gross theory description for these quantities. At first we deal with the calculation of the average beta-ray energy. This quantity $\overline{E}_\beta$ is given by summing up all the contributions from the transitions to the every final levels; namely,

$$\begin{aligned}\overline{E}_\beta &= \frac{1}{\lambda}\sum_n \lambda_n \overline{E}_\beta^{(n)} \\ &= \frac{1}{\lambda}\frac{mc^2}{\hbar}\frac{G^2}{2\pi^3}\sum_n\left[|(\Psi_n,\ \Omega_F\Psi)|^2 + \frac{C_A^2}{C_V^2}|(\Psi_n,\ \Omega_{GT}\Psi)|^2\right] \\ &\quad \times\int_1^{E_n}(E-1)F(Z+1,\ E)pE(E_n-E)^2dE\ , \qquad \ldots\ldots (12)\end{aligned}$$

where $\overline{E}_\beta^{(n)}$ represents the average beta-ray energy released at a transition feeding the n-th final level as is given by Eq. (4). The partial decay constant $\lambda_n$ is given by Eq. (5). The translation of this expression into the gross theory form is easily done in a quite parallel way to the case of the decay constant. The only difference is that the integrant, in this case, has an additional factor (E − 1) which does not appear in the expression (6) for $\lambda$.

$$\begin{aligned}\overline{E}_\beta &= \frac{C}{\lambda}\int_{-Q_\beta}^{0}\left[|M_F(E_g)|^2 + 3\frac{C_A^2}{C_V^2}|M_{GT}(E_g)|^2\right] \\ &\quad \times\left[\int_1^{-E_g+1}(E-1)\ F(Z+1,\ E)pE(-E_g+1-E)^2dE\right]dE_g\ , \qquad \ldots (13)\end{aligned}$$

where the constant C denotes the factor $\frac{mc^2}{\hbar}\ \frac{G^2}{2\pi^3}$

To derive the expression for the gamma-ray energy $\overline{E}_\gamma$ we assume that the excitation energy of the level populated by the beta-transition is released solely as gamma-rays; in other words we neglect the effects of the delayed neutron emission and the internal conversion. The expression, then becomes as

$$\overline{E}_\gamma = \frac{1}{\lambda}\sum_n \lambda_n \overline{E}_\gamma^{(n)}$$
$$= \frac{1}{\lambda}\sum_n (Q_\beta - E_n + 1)\lambda_n$$
$$= \frac{1}{\lambda}\frac{mc^2}{\hbar}\frac{G^2}{2\pi^3}\sum_n \left[ |(\Psi_n, \Omega_F \Psi)|^2 + \frac{C_A^2}{C_V^2}|(\Psi_n, \Omega_{GT}\Psi)|^2 \right]$$
$$\times (Q_\beta - E_n + 1) f(E_n) \ . \qquad \cdots\cdots\cdots \quad (14)$$

The corresponding expression in the gross theory form is

$$\overline{E}_\gamma = \frac{C}{\lambda}\int_{-Q_\beta}^{0} \left[ |M_F(E_g)|^2 + 3\frac{C_A^2}{C_V^2}|M_{GT}(E_g)|^2 \right]$$
$$\times (Q_\beta + E_g) f(-E_g + 1) dE_g \ . \qquad \cdots\cdots\cdots \quad (15)$$

Before closing this subsection we overview the behavior of the beta-strength function. Fig. 2 displays the energy profile of the beta-strength functions for the Fermi, the Gamow-Teller, and the first-forbidden transitions. The sharp peak of the Fermi strength is situated at the isobaric analog state, the eigen state of the total isospin T. This is due to the fact that the Fermi transition operator is essentially $T_x + iT_y$ which elevates the z-component of the isospin by unit one. If the total isospin is a good quantum number, the Fermi-strength becomes a delta-function at the isobaric analog state. The thin but finite width of the strength is resulted by the impurity of the isospin. In a classical term this is interpreted as follows. The Coulomb potential within a nucleus is not always uniform. The Coulomb energy change induced by a decay of a neutron into a proton, therefore, depends on the position of the decaying neutron within the nucleus. This gives rise to the spread of the Fermi strength. The Gamow-Teller strength has a broad peak around the isobaric analog state. The wide spread of the peak is caused by incommutability of the Gamow-Teller transition operator with the spin-dependent part of the nuclear force. The strength function of the first-forbidden transition has two peaks with spread widths.

Here it should be noted that only the lower tails of these strengths are energetically accessible by real beta-transitions. (This is not the case for light nuclides, where the isobaric analog state is accessible energetically). This leads to the fact that the total strength is an increasing function of energy. Though this tendency is largely cancelled out by the presence of f, a decreasing function of the excitation energy, in the expressions for $\lambda$, $\overline{E}_\beta$, and $\overline{E}_\gamma$, the high energy part of the total strength plays an important role in the following discussions.

### 2.3 A preparatory consideration

The essential quantities needed in decay heat calculations, $\lambda$, $\overline{E}_\beta$, $\overline{E}_\gamma$, are given by the expressions (6), (13) and (15). These quantities, generally, vary sensitively if the transitions to the ground or to the low-lying states are prohibited by some selection rule. In order to consider this effect of the selection rules in the calculation based on expressions (6), (13) and (15), we follow the method of Takahashi et al.[10] and introduce a parameter $Q_{00}$, which represents the energy of the lowest level to which the transition is allowed by selection rules.

In order to incorpolate the parameter $Q_{00}$ into the gross theory, the strength function is modified as

$$|M'_\omega(E_g)|^2 = \begin{cases} |M_\omega(E_g)|^2 + \delta(E_g + Q_\beta - Q_{00}) \int_{-Q_\beta}^{-Q_\beta+Q_{00}} |M_\omega(E'_g)|^2 dE'_g & (E_g \geq -Q_\beta + Q_{00}) \\ 0 \quad (-Q_\beta \leq E_g < -Q_\beta + Q_{00}) . & \end{cases} \quad \ldots\ldots\ldots (16)$$

By this modification the strength distributed over the energy range below $Q_{00}$, where the transition is prohibited, is to be concentrated at $Q_{00}$ in the form of a delta-function. Takahashi et al. applied the same value of $Q_{00}$ to all the nuclides. In the present study we tried to find the best value of $Q_{00}$ for each nuclide.

As is described in ref. 8), 19 short-lived FPs were selected from the compilation by Tobias[20] and the parameter $Q_{00}$ was determined for each nuclide so that the calculation should reproduce the Tobias' value of $\overline{E}_\beta$ and $\overline{E}_\gamma$ best. The calculations were performed with the expressions (13) and (15) where $|M_\omega(E_g)|^2$ being replaced by the modified one $|M'_\omega(E_g)|^2$. Further, the same $Q_{00}$ value was assumed for all the types of the transition, namely, Fermi, Gamow-Teller, and 1-st forbidden transitions. The results are shown in Table I. As is seen here, the gross theory reproduces the experimental values of $\overline{E}_\beta$ and $\overline{E}_\gamma$ quite well owing to the appropriate selection of $Q_{00}$ for each nuclide. The values of $Q_{00}$ scatter between 0.0 and 2.5 MeV. Figs. 4-6 display the results of the gross theory calculations with these upper and lower values of $Q_{00}$, 0.0 and 2.5 MeV, and also with $Q_{00}$ = 1.0 MeV for FPs having Q values larger than 3 MeV. In these calculations the mass number A is fixed to 90 (for even A nuclides) or to 89 (for odd A nuclides). Most of the experiment-based values of $\overline{E}_\beta$ and $\overline{E}_\gamma$ (due to Tobias, Ref. 20)) scatter between two calculated curves of $Q_{00}$ = 0.0 MeV and of $Q_{00}$ = 2.5 MeV with a few exceptions such as $^{97}Y$, $^{82}As$ and $^{92}Rb$. The curve of $Q_{00}$ = 1.0 MeV goes through amid the scattered data points, suggesting that this curve is adoptable as a good estimation of $\overline{E}_\beta$ and $\overline{E}_\gamma$ when no further information is available which helps us to find a more reliable value of $Q_{00}$. The observations in this section suggest that the range 0.0 - 2.5 MeV should be appropriate for the $Q_{00}$ variation from nuclide to nuclide.

## 2.4 Estimation of average beta- and gamma-ray energies, $\overline{E}_\beta$ and $\overline{E}_\gamma$

The goal of this chapter is to establish a reasonable method to estimate the average beta- and gamma-ray energies released per one decay of a short-lived FP nuclide. In order to use the gross theory for this purpose, we must think out a way to find the appropriate value of the parameter $Q_{00}$ of each nuclide. This section deals with the determination of the $Q_{00}$ value.

There are very many FP nuclides for which only the half-life is known, because the measurement of half-life is easier than the experimental determination of other physical characters of a short-lived nuclide. From a practical point of view, these short-lived FPs play an important role in the FP decay heat shortly after the reactor shut-down. Further, as is discussed in the later part of this report, it is often the case that theoretically estimated values of $\overline{E}_\beta$ and $\overline{E}_\gamma$ are more reliable than those based on the experimentally determined decay schemes so long as the decay schemes are incomplete from some aspects.

The half-life $t_{1/2}$ (or the decay constant $\lambda$) is a quantity which is quite sensitive to the effect of the selection rules on the ground and low-lying levels, in other words, on the value of $Q_{00}$. In this respect we can make an assumption that the information about these effects of selection rules is included in the value of $t_{1/2}$ in a implicit way. This leads to an idea to determine the value of $Q_{00}$ on the basis of the measured half-life of each nuclide.

Fig. 7 displays a comparison between calculated and experiment-based[20] values of $\overline{E}_\beta$ and $\overline{E}_\gamma$ for 34 FPs with $Q_\beta$ larger than 5 MeV. At the time of calculation, the value of the parameter $Q_{00}$ was determined for each nuclide so that the calculation might reproduce the measured half-life in the best way. In this procedure of determining the value of $Q_{00}$ the domain of the variation of this parameter was taken to be between 0.0 and 2.0 MeV for odd-odd nuclides and between 0.5 and 2.0 MeV for others.

As is seen in the preceding section, the most of the $Q_{00}$ values which were determined so as to reproduce the experimental values of $\overline{E}_\beta$ and $\overline{E}_\gamma$ lie between 0.0 and 2.5 MeV. In the present parameter survay we cut off the upper and the lower ends of this range by 0.5 MeV and adopted the range 0.5 - 2.0 MeV as is mentioned above. An exception is the odd-odd nuclide case, where a range of 0.0 - 2.0 MeV was adopted so that the transition into the ground state should be allowed. Many odd-odd nuclides have ground states of spin-parity $1^+$ which can decay to $0^+$ ground state of the daughters (even-even) by the Gamow-Teller transition ($|\Delta J|$ = 1, parity change: no).

It is clear from the comparison of Figs. 7 and 8 that the determination of $Q_{00}$ based on measured half-life is quite effective to reproduce Realistic values of $\overline{E}_\beta$ and $\overline{E}_\gamma$. The former shows the results of the $Q_{00}$ optimization mentioned above and the latter corresponds to the case where the value of $Q_{00}$ is fixed to 1.0 MeV for all the nuclides. The values of these figures are normalized so that the sum of $\overline{E}_\beta$, $\overline{E}_\gamma$ and the anti-neutrino energy should becomes 100.0. The dotted and the solid lines indicate $\overline{E}_\beta$ and $\overline{E}_\beta + \overline{E}_\gamma$, respectively.

## 3. Data for $\overline{E}_\beta$, $\overline{E}_\gamma$ and $t_{1/2}$ Adopted in the JNDC File

### 3.1 Estimated $\overline{E}_\beta$ and $\overline{E}_\gamma$ values

The JNDC Decay Heat Evaluation Working Group calculated $\overline{E}_\beta$ and $\overline{E}_\gamma$ for more than 700 nuclides including many short-lived ones on the basis of decay schemes published until 1980. The expressions (1) and (2) were used to derive these values. For short-lived ones among them, the values $\overline{E}_\beta$ and $\overline{E}_\gamma$ were also calculated by the method described in Sec. 4.2. Fig. 9 displays the results for nuclides which have $Q_\beta$ values larger than 3 MeV. Theoretical values based on the method described in Sec. 2.4 and the values from ENDF/B-IV (Δ)[2] and from Tasaka's File (∇)[5] are also shown there. It should be noted that the ENDF/B-IV and the Tasaka's File include estimated data based on relatively simple extrapolation methods. On the other hand, the JNDC data (o) are wholly derived from decay schemes; (i.e.

Fig. 7 displays a comparison between calculated and experiment-based[20) values of $\overline{E}_\beta$ and $\overline{E}_\gamma$ for 34 FPs with $Q_\beta$ larger than 5 MeV. At the time of calculation, the value of the parameter $Q_{00}$ was determined for each nuclide so that the calculation might reproduce the measured half-life in the best way. In this procedure of determining the value of $Q_{00}$ the domain of the variation of this parameter was taken to be between 0.0 and 2.0 MeV for odd-odd nuclides and between 0.5 and 2.0 MeV for others.

As is seen in the preceding section, the most of the $Q_{00}$ values which were determined so as to reproduce the experimental values of $\overline{E}_\beta$ and $\overline{E}_\gamma$ lie between 0.0 and 2.5 MeV. In the present parameter survay we cut off the upper and the lower ends of this range by 0.5 MeV and adopted the range 0.5 - 2.0 MeV as is mentioned above. An exception is the odd-odd nuclide case, where a range of 0.0 - 2.0 MeV was adopted so that the transition into the ground state should be allowed. Many odd-odd nuclides have ground states of spin-parity $1^+$ which can decay to $0^+$ ground state of the daughters (even-even) by the Gamow-Teller transition ($|\Delta J| = 1$, parity change: no).

It is clear from the comparison of Figs. 7 and 8 that the determination of $Q_{00}$ based on measured half-life is quite effective to reproduce Realistic values of $\overline{E}_\beta$ and $\overline{E}_\gamma$. The former shows the results of the $Q_{00}$ optimization mentioned above and the latter corresponds to the case where the value of $Q_{00}$ is fixed to 1.0 MeV for all the nuclides. The values of these figures are normalized so that the sum of $\overline{E}_\beta$, $\overline{E}_\gamma$ and the anti-neutrino energy should becomes 100.0. The dotted and the solid lines indicate $\overline{E}_\beta$ and $\overline{E}_\beta + \overline{E}_\gamma$, respectively.

## 3. Data for $\overline{E}_\beta$, $\overline{E}_\gamma$ and $t_{1/2}$ Adopted in the JNDC File

### 3.1 Estimated $\overline{E}_\beta$ and $\overline{E}_\gamma$ values

The JNDC Decay Heat Evaluation Working Group calculated $\overline{E}_\beta$ and $\overline{E}_\gamma$ for more than 700 nuclides including many short-lived ones on the basis of decay schemes published until 1980. The expressions (1) and (2) were used to derive these values. For short-lived ones among them, the values $\overline{E}_\beta$ and $\overline{E}_\gamma$ were also calculated by the method described in Sec. 4.2. Fig. 9 displays the results for nuclides which have $Q_\beta$ values larger than 3 MeV. Theoretical values based on the method described in Sec. 2.4 and the values from ENDF/B-IV ($\Delta$)[2) and from Tasaka's File ($\nabla$)[5) are also shown there. It should be noted that the ENDF/B-IV and the Tasaka's File include estimated data based on relatively simple extrapolation methods. On the other hand, the JNDC data (o) are wholly derived from decay schemes; (i.e.

all the JNDC values are based on experiments.) A survey of Fig. 9 leads to the following observations; 1). The average beta-energies from the four data sources (JNDC, ENDF/B-IV, Tasaka and theoretical estimation) are consistent each other in a relative sense. 2) For the gamma-ray energy the consistency deteriorates appreciably. 3) As for the gamma-energy ($\overline{E}_\gamma$), the JNDC value is quite often the lowest among the four data sources.

A comment is needed here about the second observation above. For simplicity let us assume that the whole beta-strength concentrates on the level at $Q_{00}$. A shift of $Q_{00}$ by $\Delta Q_{00}$ results in a change in the average gamma-ray energy by the same amount, namely, by $\Delta Q_{00}$. On the contrary the average beta-energy changes only by C $Q_{00}$, where the factor C, having a value smaller than 1.0 (0.3 - 0.5), is the ratio of the beta-ray energy to the sum of beta-ray and anti-neutrino energies. In this respect $\overline{E}_\gamma$ is more sensitive to the assumed value of $Q_{00}$ than the case of $\overline{E}_\beta$. In the estimation calculations of $\overline{E}_\beta$ and $\overline{E}_\gamma$, the assumed values of $Q_{00}$ have fairly large ambiguity in general. Hence the estimated value of $\overline{E}_\gamma$ is more ambiguous than the value of $\overline{E}_\beta$.

3.2 Data for $\overline{E}_\beta$, $\overline{E}_\gamma$ and $t_{1/2}$ for nuclides with no experimental data

Among more than 1100 nuclides and isomers whose decay and yield data are stored in the JNDC FP Decay Data File, about 380 nuclides and isomers lack measured decay data. More precisely, neither half-lives nor decay schemes are known for 280 among them, and only half-lives are known for the rest. Theoretical estimation of $\overline{E}_\beta$, $\overline{E}_\gamma$ and $t_{1/2}$ were carried out for these nuclides with the aid of the gross theory and the results were stored into the JNDC FP Decay Data File.

1) Estimation of $\overline{E}_\beta$ and $\overline{E}_\gamma$ for nuclides with no decay data except $t_{1/2}$:
For these nuclides the values of $\overline{E}_\beta$ and $\overline{E}_\gamma$ were estimated with the method described in Sec. 2.4. The parameter $Q_{00}$ was optimized so that the best consistency should be attained between calculated and measured half-lives. The variation range of $Q_{00}$ was taken to be $0.0 \le Q_{00} \le 2.0$ MeV for odd-odd nuclides and to be $0.5 \le Q_{00} \le 2.0$ MeV for others. The $Q_\beta$ values were taken from the compilation by Wapstra and Bos,[23)] or were calculated by Uno and Yamada's linear type mass formula[24)] when Wapstra and Bos give no information. Table II summarizes the values of $\overline{E}_\beta$, $\overline{E}_\gamma$, $Q_\beta$ and $Q_{00}$ for the nuclides belonging to this category.
2) Estimation of $\overline{E}_\beta$, $\overline{E}_\gamma$ and $t_{1/2}$ for nuclides with no measured data:

For these nuclides, the estimation method used for the nuclides of category 1) is inapplicable because half-lives are not known. The key parameter $Q_{00}$ was determined in the following two methods, namely;
(a) The $Q_{00}$-value was fixed to 1.0 MeV for all the nuclides.
(b) Systematic behavior of the values of $Q_{00}$ was examined in several subdivided mass regions and the value of $Q_{00}$ was extrapolated to each nuclide in each mass region.

By use of the $Q_{00}$ values determined in the above two methods, $\overline{E}_\beta$, $\overline{E}_\gamma$ and $t_{1/2}$ were calculated. There was, however, no essential difference between the two decay heat curves corresponding to the above two methods. This is due to the fact that the contribution from the nuclides of this category is minor even at very short cooling-times. In practice we stored the $\overline{E}_\beta$, $\overline{E}_\gamma$ and $t_{1/2}$ data based on method (b). The whole results are given in Table III.

### 3.3 Adoption of theoretical data for high-$Q_\beta$ nuclides with experimental data

For 88 short-lived nuclides listed in Table IV, theoretically estimated values of $\overline{E}_\beta$ and $\overline{E}_\gamma$ were finally adopted, though these nuclides have experimental information on their beta- and gamma-decay schemes which enable us to calculate $\overline{E}_\beta$ and $\overline{E}_\gamma$ apart from their reliability. A justification for this preferential adoption of the theoretical data in place of the experiment-based data will be dealt with in Chapter 4. The method to obtain the theoretical values of $\overline{E}_\beta$ and $\overline{E}_\gamma$ is the same as that for the nuclides of category 1) of Sec. 3.2; namely, the optimization of the parameter $Q_{00}$ with the aid of the measured half-life. Table IV summarizes the theoretical (T) and experiment-based (E) values of $\overline{E}_\beta$ and $\overline{E}_\gamma$, the measured half-lives used to determine $Q_{00}$, the resultant value of $Q_{00}$ and the calculated half-lives. This table also gives fractional contribution from each nuclide in the $^{235}U$ decay heat shortly after a burst irradiation of thermal neutrons.

Before ending this chapter we review briefly the consequence of this adoption of the theoretical data though detailed descriptions are given in Ref. 25). Figs. 10 and 11 display the beta- and gamma-ray components of the $^{235}U$ decay heat after an instantaneous irradiation of thermal neutrons. Adoption of the theoretically estimated values of $\overline{E}_\beta$ and $\overline{E}_\gamma$ for the above 88 nuclides drastically improves the consistency between the calculated and the measured decay heat (from Ⓐ to Ⓑ ). LaVauve et al. successfully tried to remove an apparent disagreement between measured and calculated decay heat curves at short cooling time by introducing the JNDC values of $\overline{E}_\beta$ and $\overline{E}_\gamma$ into the ENDF/B-V data base.[30] Their results are shown in Fig. 12. Remarkable change brought about by the introduction of the JNDC data seems to come mostly from the 88 nuclides described above in their result, too. In the next chapter we see the reason why the theoretical values lead to a success in interpreting the measured decay heat at short cooling-times.

## 4. Problems in Deriving $\overline{E}_\beta$ and $\overline{E}_\gamma$ from Decay Schemes

### 4.1 Incompleteness of decay schemes for short-lived nuclides

A quite suggestive numerical experiment was carried out by J. C. Hardy et al.[31] They generated numerically a hypothetical beta-gamma decay scheme of a fictional nuclide 'pandemonium' under the following conditions.

1) Atomic and mass numbers and spin-parity are taken to be the same as Gd-145, namely z = 64, A = 145, $I^\pi = 1/2^+$ and further $Q_{EC}$ = 5 MeV.
2) The level density of the daughter nuclide (Z = 63, A = 145) takes after the Gilbert-Cameron's level density formula.
3) Level spacings obey the Wigner's statistics.
4) The Gamow-Teller transition probability to each level obeys the random Porter-Thomas distribution.
5) The beta-transition matrix is assumed to be independent of the excitation energy.

Then the Ge(Li)-detector response to the gamma-rays from the decaying 'pandemonium' was generated under realistic conditions for resolution, efficiency, etc. The resultant response data were analysed with a peak analysis code SAMPO. As a result of this gedanken-experiment it was proved that a sizable portion of the total gamma-ray intensity remained undetected. From this observation they concluded that the decay schemes constructed on the basis of the peak analysis and the intensity balance of gamma-rays are incomplete in general for short-lived high-Q-value nuclides. They do not describe this incompleteness of decay schemes in detail. It is easy to see, however, that the incompleteness manifests itself in the high excitation-energy side where the level density is high and the gamma decay structure is complicated. When the high energy part of a decay scheme is oversimplified or missing, the beta-strength function is underestimated at high energy. This inevitably introduces a systematic bias into the values of $\overline{E}_\beta$ and $\overline{E}$ . This must be the origin of the overestimation of the beta decay-heat and the underestimation of the gamma decay-heat at short cooling calculated decay heat curves at short cooling time by introducing the JNDC values of $\overline{E}_\beta$ and $\overline{E}_\gamma$ into the ENDF/B-V data base.[30] Their results are shown in Fig. 12. Remarkable change brought about by the introduction of the JNDC data seems to come mostly from the 88 nuclides described above in their result, too. In the next chapter we see the reason why the theoretical values lead to a success in interpreting the measured decay heat at short cooling-times.

## 4. Problems in Deriving $\overline{E}_\beta$ and $\overline{E}_\gamma$ from Decay Schemes

### 4.1 Incompleteness of decay schemes for short-lived nuclides

A quite suggestive numerical experiment was carried out by J. C. Hardy et al.[31] They generated numerically a hypothetical beta-gamma decay scheme of a fictional nuclide 'pandemonium' under the following conditions.

1) Atomic and mass numbers and spin-parity are taken to be the same as Gd-145, namely z = 64, A = 145, $I^\pi = 1/2^+$ and further $Q_{EC}$ = 5 MeV.
2) The level density of the daughter nuclide (Z = 63, A = 145) takes after the Gilbert-Cameron's level density formula.
3) Level spacings obey the Wigner's statistics.
4) The Gamow-Teller transition probability to each level obeys the random Porter-Thomas distribution.
5) The beta-transition matrix is assumed to be independent of the excitation energy.

Then the Ge(Li)-detector response to the gamma-rays from the decaying 'pandemonium' was generated under realistic conditions for resolution, efficiency, etc. The resultant response data were analysed with a peak analysis code SAMPO. As a result of this gedanken-experiment it was proved that a sizable portion of the total gamma-ray intensity remained undetected. From this observation they concluded that the decay schemes constructed on the basis of the peak analysis and the intensity balance of gamma-rays are incomplete in general for short-lived high-Q-value nuclides. They do not describe this incompleteness of decay schemes in detail. It is easy to see, however, that the incompleteness manifests itself in the high excitation-energy side where the level density is high and the gamma decay structure is complicated. When the high energy part of a decay scheme is oversimplified or missing, the beta-strength function is underestimated at high energy. This inevitably introduces a systematic bias into the values of $\overline{E}_\beta$ and $\overline{E}$ . This must be the origin of the overestimation of the beta decay-heat and the underestimation of the gamma decay-heat at short cooling times, which was depicted in section 3.3.

Fig. 13 displays a decay scheme of $^{93}Kr$, which is taken from the Tables of Isotopes 7th edition.[22] This nuclide, situated near the light peaks of the fission yield curves of U and Pu, has a relatively high $Q_\beta$-value (7.3 MeV[22] - 8.7 MeV[6]) and a short beta half-life. The excited levels are identified, however, only up to 4.9392 MeV and 98.1 % of the total beta-intensity is allotted below this highest level. It seems unreal that there is no beta-intensity between 5 and 7 MeV. Actually 1.9 % of the beta-intensity is given to the delayed neutron window around 7 MeV. This intensity happened to be detected owing to the existence of the delayed neutron, which played a role of a probe, so to speak. It is, therefore, doubtless that a non-negligible amount of beta-intensity should exist between 5 and 7 MeV, and also above 7 MeV. The $\overline{E}_\beta$ value is over-estimated and the $\overline{E}_\gamma$ value is underestimated when they are derived from this decay scheme which lacks beta-intensities to unknown highly excited levels. This example of $^{93}Kr$ is not a exceptional one but represents a defect common to high-$Q_\beta$-value decay schemes. As another example, let examine the case of $^{95}Sr$, which has a $Q_\beta$-value of 6.09 MeV[22] (Fig. 14). In this case no beta-intensity is given above 4.2677 MeV. The $\overline{E}_\beta$ and $\overline{E}_\gamma$ values are as follows.

| | $\overline{E}_\beta$ (Beta-energy) | | $\overline{E}_\gamma$ (Gamma-energy) | |
|---|---|---|---|---|
| | Decay scheme | Gross theory | Decay scheme | Gross theory |
| $^{93}Kr$ | 2.89 | 2.73 | 2.28 | 2.76 |
| $^{95}Sr$ | 2.27 | 1.59 | 1.03 | 2.44 |

(all in MeV unit)

When being derived from decay schemes, $\overline{E}_\beta$ is larger and $\overline{E}_\gamma$ is smaller in comparison with the gross theory values as is expected from the above discussion. It should be kept in mind, however, that the gross theory does not always give the best estimates of $\overline{E}_\beta$ and $\overline{E}_\gamma$ for each individual nuclide, because this theory describes overall properties of wide range of nuclides from its nature.

Observations in this section can be summarized in the following way. The published decay schemes of short-lived FPs miss a non-negligible amount of the beta-intensity to unknown highly-excited levels. This leads to an overestimation of $\overline{E}_\beta$ and, equivalently, to an underestimation of $\overline{E}_\gamma$. In this defect of the published decay schemes we find the reason why the recently completed libraries such as the preliminary version of the JNDC file, ENDF/B-V[30] and UKFPDD-2[32] failed in reproducing the beta- and gamma-ray components of decay heat at short cooling-times.

4.2 Beta-strength function and decay heat

In section 4.1 we dealt with incompleteness of high-$Q_\beta$-value decay schemes and with its consequences on derived $\overline{E}_\beta$ and $\overline{E}_\gamma$ values. In this section a quite simple strength function model is introduced in order to make the discussion more quantitative.

In recent years information on the beta-strength functions has been accumulated by using of specially designed instrumentations.[33)-35)] Fig. 15 displays beta-strength functions of short-lived FPs measured by K. H. Johansen et al.[34)] Difference between the open and the solid circles comes from the uncertainty in assumed $Q_\beta$-values. Very roughly speaking we can fit these curves with an exponential function $e^{E/\alpha}$. The value of $\alpha$ ranges from 0.5 to 2.0 MeV. This observation will be made use in the later part of this section.

The average gamma-ray energy $\overline{E}_\gamma$ can be expressed as (15) in terms of the strength functions. We use an energy variable E (equivalent to $\varepsilon$ used in chapter 2) instead of $E_g$. They are related as $E = Q_\beta + E_g$. Then, we have

$$\overline{E}_\gamma = \frac{C}{\lambda}\int_0^{Q_\beta} |M(E - Q_\beta)|^2 E \int_1^{Q_\beta - E + 1} F(Z + 1, W)(W^2 - 1)^{1/2} W(Q_\beta - E + 1 - W)^2 dW dE\,, \quad \cdots\cdots\cdots \quad (17)$$

where the integrated Fermi function f is rewritten explicitly using the expression (5'). We confine the following discussion within the allowed transition. Hence the Fermi function F(Z,W) is written in non-relativistic approximation as[36)]

$$F(Z, W) = \frac{2\pi y}{1 - \exp(-2\pi y)}\,, \qquad y = \frac{Z}{137} W(W^2 - 1)^{-1/2}\,.$$

Further, by using of an approximation $F(Z, W) \approx 2\pi y$, the integrant of the second integral becomes $W^2(Q_\beta - E + 1 - W)^2$ and analytically integrable. The result is $(X^5 + 5X^4 + 10X^3)/30$ with $X = Q_\beta - E$. By rewriting $|M(E - Q_\beta)|^2$ as $S_\beta(E)$, we get a simple expression for average gamma-ray energy;

$$\overline{E}_\gamma = \frac{C}{30\lambda}\int_0^{Q_\beta} S_\beta(E)E(X^5 + 5X^4 + 10X^3)dE \quad . \quad . \quad . \quad . \quad . \quad . \quad . \quad . \quad (18)$$

It is shown that the above approximations for the Fermi function introduce no serious error except heavy nuclides like actinides.[37] By using of the expression (18), the consequences of the missing beta-intensity to the highly excited levels will be examined.

Let us suppose two types of the energy dependence of the beta-strength function; linear type $S_\beta \propto E$ and exponential type $S_\beta \propto e^{E/\alpha}$. In order to see the effect of the missing beta-intensity, or the missing strength, we introduce a modified strength function $S_\beta(E, q)$, which has no strength above a critical energy q,

$$S_\beta(E, q) = \begin{cases} C_s E \text{ or } C_s e^{E/\alpha} & \text{for } 0 \le E < q \\ 0 & \text{for } q \le E \le Q_\beta \ . \end{cases}$$

The function $S_\beta(E, Q_\beta)$ represents a situation in which the strength is fully known up to the maximum excitation energy. We write the average gamma-ray energy as $\overline{E}_\gamma(q)$ which is calculated with the strength $S_\beta(E, q)$;

$$\overline{E}_\gamma(q) \quad \frac{\int_0^{Q_\beta} S_\beta(E, q)E(X^5 + 5X^4 + 10X^3)dE}{\int_0^{Q_\beta} S_\beta(E, q)(X^5 + 5X^4 + 10X^3)dE} \quad . \quad . \quad . \quad . \quad . (19)$$

$$(X = Q_\beta - E) \ .$$

The ratio $\overline{E}_\gamma(q)/\overline{E}_\gamma(Q_\beta)$ gives a measure of the underestimation of $\overline{E}_\gamma$ caused by missing of beta-intensity above the energy q. Fig. 16 displays this ratio as a function of q on the basis of three types of assumed strength functions; E, $e^{E/1.5}$ and $e^E$. The experimental background of taking the value of $\alpha$ to be 1.5 and 1.0 MeV is as follows.

1) As was observed at the beginning of this section the value of $\alpha$ ranges from 0.5 to 2.0 MeV.
2) The ratio $\overline{E}_\gamma/Q_\beta$ should fall within 0.25 - 0.35, which is a typical value of this ratio from the viewpoint of the microscopic and integral measurements. (See Table V)

Among the values of $\alpha$ which fulfil the above criteria, two typical values, 1.5 and 1.0 MeV, were adopted for the present discussion. As is seen from Table V, $\overline{E}_\gamma/Q_\beta$ is too large for large $Q_\beta$ nuclides when $S_\beta \propto e^{E}$ is used. From this respect, $S_\beta \propto e^{E/1.5}$ is preferable. (See footnote 3)

Let us examine the curve in Fig. 16, which corresponds to $Q_\beta$ = 8 MeV and $S_\beta \propto e^{E/1.5}$. If the beta transition to levels above 5 MeV is missed, the $\overline{E}_\gamma$ value is underestimated by 10 %. This reaches 20 % when the intensity is missing above 4 MeV. The underestimation becomes larger if we take $e^{E}$ as $S_\beta$. A survey of published decay schemes of short-lived FPs (typically refer to the Tables of Isotopes[22]) leads to an observation that beta-intensity is not given above 3 - 5 MeV for most high-$Q_\beta$ nuclides. By combining this observation with the above result from the simple strength-function calculation, we come to a conclusion that the value of $\overline{E}_\gamma$ is open to underestimation by 10 - 30 % for nuclides with $Q_\beta$-values larger than 5 - 6 MeV. On the contrary the $\overline{E}_\gamma$ and $\overline{E}_\beta$ values calculated with the gross theory reflect properly the effect of the large beta-strength at high energy, which increases $\overline{E}_\gamma$ and decreases $\overline{E}_\beta$.[note 4)] This is the reason why the introduction of gross theory values drastically improved the reproducibility of the measured beta- and gamma-ray components of the decay heat at short cooling-times.

## 5. Concluding Remarks

The method of theoretical estimation of the average energies $\overline{E}_\beta$ and $\overline{E}_\gamma$ was described in detail. It is a notable feature of the JNDC FP Decay Data File that these estimated values are fully adopted for short-lived FPs with high $Q_\beta$-values ($Q_\beta \gtrsim$ 5 MeV) in place of the values derived from the published decay schemes. Discussions were made in favor of this preferential selection of the theoretical values. In the course of the discussions the following things were known.

Note 3) Several authors assumed a level-density-proportional behavior for the beta-strength function. Roughly speaking, this assumption corresponds to taking the $\alpha$ value as 0.5 - 0.9 in the expression $S_\beta \propto e^{E/\alpha}$. This selection, however, leads to serious overestimation of $\overline{E}_\gamma/Q_\beta$ ratio (larger than 0.4). Further, this ratio increases too rapidly as a function of $Q_\beta$. From this respect, the level-density proportional assumption is not acceptable.

Note 4) Here consideration was made only for $\overline{E}_\gamma$. It is easy to see, however, $\overline{E}_\beta$ is overestimated when $\overline{E}_\gamma$ is underestimated, for they are closely related by the energy conservation.

1.5 and 1.0 MeV, were adopted for the present discussion. As is seen from Table V, $\overline{E}_\gamma/Q_\beta$ is too large for large $Q_\beta$ nuclides when $S_\beta \propto e^{E}$ is used. From this respect, $S_\beta \propto e^{E/1.5}$ is preferable. (See footnote 3)

Let us examine the curve in Fig. 16, which corresponds to $Q_\beta$ = 8 MeV and $S_\beta \propto e^{E/1.5}$. If the beta transition to levels above 5 MeV is missed, the $\overline{E}_\gamma$ value is underestimated by 10 %. This reaches 20 % when the intensity is missing above 4 MeV. The underestimation becomes larger if we take $e^{E}$ as $S_\beta$. A survey of published decay schemes of short-lived FPs (typically refer to the Tables of Isotopes[22]) leads to an observation that beta-intensity is not given above 3 - 5 MeV for most high-$Q_\beta$ nuclides. By combining this observation with the above result from the simple strength-function calculation, we come to a conclusion that the value of $\overline{E}_\gamma$ is open to underestimation by 10 - 30 % for nuclides with $Q_\beta$-values larger than 5 - 6 MeV. On the contrary the $\overline{E}_\gamma$ and $\overline{E}_\beta$ values calculated with the gross theory reflect properly the effect of the large beta-strength at high energy, which increases $\overline{E}_\gamma$ and decreases $\overline{E}_\beta$.[note 4)] This is the reason why the introduction of gross theory values drastically improved the reproducibility of the measured beta- and gamma-ray components of the decay heat at short cooling-times.

## 5. Concluding Remarks

The method of theoretical estimation of the average energies $\overline{E}_\beta$ and $\overline{E}_\gamma$ was described in detail. It is a notable feature of the JNDC FP Decay Data File that these estimated values are fully adopted for short-lived FPs with high $Q_\beta$-values ($Q_\beta \gtrsim$ 5 MeV) in place of the values derived from the published decay schemes. Discussions were made in favor of this preferential selection of the theoretical values. In the course of the discussions the following things were known.

---

Note 3) Several authors assumed a level-density-proportional behavior for the beta-strength function. Roughly speaking, this assumption corresponds to taking the α value as 0.5 - 0.9 in the expression $S_\beta \propto e^{E/\alpha}$. This selection, however, leads to serious overestimation of $\overline{E}_\gamma/Q_\beta$ ratio (larger than 0.4). Further, this ratio increases too rapidly as a function of $Q_\beta$. From this respect, the level-density proportional assumption is not acceptable.

Note 4) Here consideration was made only for $\overline{E}_\gamma$. It is easy to see, however, $\overline{E}_\beta$ is overestimated when $\overline{E}_\gamma$ is underestimated, for they are closely related by the energy conservation.

1) The beta-strength function increases with the excitation energy of the final state. In calculations of $\overline{E}_\beta$, $\overline{E}_\gamma$ and $t_{1/2}$, the effect of this increasing trend of $S_\beta$ is cancelled out to a large extent by the presence of the Fermi-function which decreases rapidly with the energy. In order to calculate the average energies $\overline{E}_\beta$ and $\overline{E}_\gamma$ accurately, however, it is quite important to take the effect of the increasing strength into account.

2) Published decay schemes of high $Q_\beta$-value nuclides are usually constructed on the basis of the intensity balance of gamma-ray spectra. Generally speaking, there exist quite many types of gamma-rays emitted at the time of beta-decay of a high-$Q_\beta$ nuclide because the structure of the high energy final levels is complex and dense. A sizable portion of these gamma-rays remain undetected due to weakness of their intensity. It also happens that some gamma-rays are not placed in appropriate positions in the decay scheme although they are detected. These lead to missing of high energy levels, in other words, to missing of beta-strength at high energy. This is the reason why $\overline{E}_\beta$ is overestimated and $\overline{E}_\gamma$ is underestimated when they are derived from decay schemes.

3) Full adoption of the theoretical values of $\overline{E}_\beta$ and $\overline{E}_\gamma$ drastically improved the agreement between calculation and measurement for both beta- and gamma-ray components of decay heat at short cooling-times. This fact indicates that the gross theory predicts reasonably well the energy behavior of the beta-strength function on an average over some range of nuclides.

## Acknowledgments

The author expresses deep thanks to Profs. R. Nakasima and M. Yamada for their valuable comments, and to Dr. Z. Matumoto for critical reading of the manuscript. He is much indebted also to Drs. M. Akiyama, K. Tasaka and Mr. H. Ihara.

1) The beta-strength function increases with the excitation energy of the final state. In calculations of $\overline{E}_\beta$, $\overline{E}_\gamma$ and $t_{1/2}$, the effect of this increasing trend of $S_\beta$ is cancelled out to a large extent by the presence of the Fermi-function which decreases rapidly with the energy. In order to calculate the average energies $\overline{E}_\beta$ and $\overline{E}_\gamma$ accurately, however, it is quite important to take the effect of the increasing strength into account.

2) Published decay schemes of high $Q_\beta$-value nuclides are usually constructed on the basis of the intensity balance of gamma-ray spectra. Generally speaking, there exist quite many types of gamma-rays emitted at the time of beta-decay of a high-$Q_\beta$ nuclide because the structure of the high energy final levels is complex and dense. A sizable portion of these gamma-rays remain undetected due to weakness of their intensity. It also happens that some gamma-rays are not placed in appropriate positions in the decay scheme although they are detected. These lead to missing of high energy levels, in other words, to missing of beta-strength at high energy. This is the reason why $\overline{E}_\beta$ is overestimated and $\overline{E}_\gamma$ is underestimated when they are derived from decay schemes.

3) Full adoption of the theoretical values of $\overline{E}_\beta$ and $\overline{E}_\gamma$ drastically improved the agreement between calculation and measurement for both beta- and gamma-ray components of decay heat at short cooling-times. This fact indicates that the gross theory predicts reasonably well the energy behavior of the beta-strength function on an average over some range of nuclides.

## Acknowledgments

The author expresses deep thanks to Profs. R. Nakasima and M. Yamada for their valuable comments, and to Dr. Z. Matumoto for critical reading of the manuscript. He is much indebted also to Drs. M. Akiyama, K. Tasaka and Mr. H. Ihara.

References

1) Devillers C. et al., 'Bibliotheque de Données Relatives aux Produits de Fission', Proc. Symp. Application of Nuclear Data in Science and Technol., SM-170/63, International Atomic Energy Agency (1973)

2) Evaluated Nuclear Data File, ENDF/B-IV, National Nuclear Data Center, Brookhaven National Lab., see also T. R. England, R. E. Schenter, 'ENDF/B-IV Fission-Product Files: Summary of Major Nuclide Data', LA-6116-MS, Los Alamos Scientific Lab., (1975)

3) Evaluated Nuclear Data File, ENDF/B-V, ibid.

4) Tobias, A., Davies, B. S. J., 'A Revised Fission Product Decay Data File in ENDF/B-IV Format', RD/B/N4942, CEGB report (1980)

5) Tasaka, K., 'Nuclear Data Library of Fission Products for Decay Heat Calculation', NUREG/CR-0705 (1979)

6) Yamamoto, T., Akiyama, M., Matumoto, Z., Nakasima, R., 'JNDC FP Decay Data File', JAERI-M 9357 (1981)

7) Schmittroth, F., Schenter, R. E., Nucl. Sci. Engn., 63, 276 (1977)

8) Yoshida, T., Nucl. Sci. Engn., 63, 376 (1977)

9) Takahashi, K., Yamada, M., Progr. Theor. Phys., 41, 1470 (1969); Koyama, S., Takahashi, K., Yamada, M., ibid., 44, 663 (1970); Takahashi, K., ibid., 45, 1466 (1971)

10) Takahashi, K., Yamada, M., Kondoh, T., At. Nucl. Data Tables, 12, 101 (1973)

11) Wu, C. H., 'Average Beta and Gamma Decay Energies of the Fission Products', PhD Thesis, Oregon State University (1979)

12) Schmittroth, F., 'Theoretical Estimation of Decay Information for Non-experimental Nuclides', Conf. on Nucl. Data Evaluation Methods and Procedures, Brookhaven National Laboratory (1980)

13) Klapdor, H. V., Oda, T., Astrophys. J., 242 (1980)

14) Yamada, M., Morita, M., Fujii, J., 'Beta Decay and Weak Interactions', Baifu-kan (1974) (in Japanese)

15) Yamada, M., Bull. Sci. Eng. Lab., Waseda University, No. 31/32, 146 (1965)

16) Takahashi, K., Yamada, M., Progr. Theor. Phys., 41, 1470 (1969)

17) Takahashi, K., Progr. Theor. Phys., 45, 1466 (1971)

18) Koyama, S., Takahashi, K., Yamada, M., Progr. Theor. Phys., 44, 663 (1970)

19) For example, Bohr, A., Mottelson, B. R., 'Nuclear Structure', Vol. I, W. A. Benjamin, Inc. (1969) p. 46

20) Tobias, A., 'Data for the Calculation of Gamma Radiation Spectra and Beta Heating from Fission Products', RD/B/M2669, U. K. Central Electricity Generating Board (1973)

21) Yoshida, T., 'GROSS-M and GROSS-P, Code for Prediction of Beta-Decay Properties and the Evaluation of their Applicability to Decay Heat Calculations', JAERI-M6313 (1975)

22) Lederer, C. M. et al., Tables of Isotopes, 7-th edition (1979) John Wiley & Sons

23) Wapstra, A. H., Bos, K., 'The 1977 Atomic Mass Evaluation', Atomic Data and Nuclear Data Tables, 19, 215 (1977)

24) Uno, M., Yamada, M., Atomic Mass and Fundamental Constants 6, edited by J. A. Nolen, W. Benenson, Plenum Publishing Co., New York, (1980) p. 141; see also, Ando, Y., Uno, M., Yamada, M., 'Prediction of Mass Excess, β-decay Energy and Neutron Separation Energy from the Atomic Mass Formula with Empirical Shell Terms', JAERI-M 83-025 (1983)

25) Yoshida, T., Nakasima, R., J. Nucl. Sci. Technol., 18(6), 393 (1971)

26) Dickens, J. K., Love, T. A., McConnell, J. W., Peelle, R. W., Nucl. Sci. Engn., 74, 106 (1980)

27) MacMahon, T. D., Wellum, R., Wilson, H. W., J. Nucl. Energy, 24, 493 (1970)

28) Perry, A. M., Maienschein, F. C., Vondy, D. R., 'Fission Product After Heat - A Review of Experiment Pertinent to the Thermal-Neutron Fission of U-235', ORNL-TM-4197 (1973)

29) Fischer, P. C., Engel, L. B., Phys. Rev., 134, B796 (1964)

30) LaBauve, R. J., England, T. R., George, D. C., 'Integral Data Testing of ENDF/B Fission Product Data and Comparison of ENDF/B with Other Fission Product Data Files, LA-9090-MS (ENDF-320), (1981)

31) Hardy, J. D., Carraz, L. C., Jonson, B., Hansen, P. G., Phys. Lett., 71B, 307 (1977)

32) Tobias, A., 'Decay Heat Summation Calculations using UKFPDD-2', RD/B/N4949, U. K. Central Electricity Generating Board (1980)

33) Hansen, P. G., Advances in Nucl. Phys., 7, 159 (1974)

34) Johansen, K. H., Bonde Nielsen, K., Rudstam, G., Nucl. Phys., A203, 481 (1973)

35) Aleklett, K., Nyman, G., Rudstam, G., Nucl. Phys., A246, 425 (1975)

36) Konopinski, E. J., 'The Theory of Beta Radioactivity', Oxford University Press (1966) p.12

37) Stamatelatos, M. G., England, T. R., Nucl. Sci. Engn., 63, 204 (1977)

38) Yamamoto, T., Sugiyama, K., Annals of Nucl. Engy., 5, 621 (1978)

39) Rudstam, G., Grapengiesser, B., Lund, E., Contribution to Review Paper No. 12, Panel on FP Nucl. Data, Bologna, IAEA (1973)

TABLE I

Average beta- and gamma-ray energies from short-lived FPs

(Parameter $Q_{00}$ determined to reproduce the experimental values)
[Upper = experimental (Ref. 4); lower = calculated]

| *A* | *Z* | Element | Even-Odd | Beta-Particle Energy (MeV) | Gamma-Ray Energy (MeV) | $Q_{00}$ | Q Value (MeV) |
|---|---|---|---|---|---|---|---|
| 76 | 31 | Ga | o-o | 1.675<br>1.684 | 2.808<br>2.794 | 2.0 | 6.610 |
| 80 | 33 | As | o-o | 2.468<br>2.471 | 0.554<br>0.578 | 0.2 | 5.999 |
| 82 | 33 | As | o-o | 3.137<br>2.952 | 0.336<br>0.760 | 0.0 | 7.146 |
| 86 | 35 | Br | o-o | 1.765<br>1.783 | 3.296<br>3.266 | 2.5 | 7.296 |
| 87 | 35 | Br | o-e | 2.087<br>2.076 | 1.727<br>1.737 | 1.3 | 6.362 |
| 89 | 36 | Kr | e-o | 1.231<br>1.215 | 2.072<br>2.109 | 1.9 | 4.971 |
| 90 | 37 | Rb | o-o | 1.789<br>1.803 | 2.559<br>2.550 | 1.7 | 6.624 |
| 91 | 36 | Kr | e-o | 2.000<br>2.030 | 0.748<br>0.764 | 0.4 | 5.298 |
| 91 | 37 | Rb | o-e | 1.320<br>1.299 | 2.871<br>2.804 | 2.5 | 5.844 |
| 92 | 36 | Kr | e-e | 2.700<br>2.601 | 0.751<br>0.927 | 0.0 | 6.615 |
| 92 | 37 | Rb | o-o | 3.714<br>3.127 | 0.260<br>1.467 | 0.0 | 8.216 |
| 93 | 38 | Sr | e-o | 0.784<br>0.795 | 2.135<br>2.075 | 2.0 | 4.054 |
| 95 | 39 | Y | o-e | 1.713<br>1.732 | 0.523<br>0.527 | 0.3 | 4.464 |
| 97 | 39 | Y | o-e | 1.612[a]<br>2.075 | 0.935<br>1.501 | 1.0 | 6.135 |
| 100 | 41 | $Nb^m$ | o-o | 2.023<br>2.035 | 1.942<br>1.978 | 1.0 | 6.538 |
| 116 | 47 | Ag | o-o | 2.185<br>2.222 | 0.710<br>0.744 | 0.0 | 5.710 |
| 132 | 51 | Sb | o-o | 1.664<br>1.698 | 2.006<br>2.007 | 0.9 | 5.922 |
| 134 | 51 | Sb | o-o | 2.879<br>2.802 | 2.026<br>2.295 | 0.0 | 8.482 |
| 136 | 53 | I | o-o | 1.808<br>1.839 | 1.911<br>1.920 | 0.7 | 6.137 |

[a]The ENDF/B-IV file gives 2.162 MeV.

Table II   Average β- and γ-ray Energies for $t_{1/2}$-known Nuclides (Gross Theory)

| NUCLIDE | E-BETA (MEV) | E-GAMMA (MEV) | Q-VALUE (MEV) | HALF-LIFE (SEC) | NUCLIDE | E-BETA (MEV) | E-GAMMA (MEV) | Q-VALUE (MEV) | HALF-LIFE (SEC) |
|---|---|---|---|---|---|---|---|---|---|
| CU 68M | 0.197 | 0.956 | 1.414 | 225.000 | BR 88 | 2.454 | 3.210 | 8.600 | 16.300 |
| CU 70M | 1.650 | 2.167 | 6.310 | 46.000 | RB 88 | 1.193 | 2.494 | 5.309 | 1068.000 |
| CU 70 | 2.697 | 0.295 | 6.170 | 4.500 | SE 89 | 3.126 | 1.894 | 8.630 | 0.410 |
| GA 74 | 1.288 | 2.401 | 5.400 | 495.000 | BR 89 | 2.373 | 2.728 | 8.040 | 4.380 |
| ZN 75 | 2.143 | 0.870 | 5.620 | 10.200 | SE 90 | 2.904 | 2.633 | 7.470 | 0.600 |
| ZN 76 | 1.398 | 0.754 | 3.980 | 5.700 | BR 90 | 3.089 | 3.662 | 10.330 | 1.920 |
| GA 76 | 1.746 | 2.496 | 6.770 | 27.100 | RB 90 | 1.571 | 2.759 | 6.360 | 153.000 |
| ZN 77 | 2.635 | 1.171 | 6.910 | 1.400 | RB 90M | 1.544 | 2.666 | 6.193 | 258.000 |
| GA 77 | 2.043 | 0.789 | 5.180 | 13.000 | SE 91 | 3.785 | 3.126 | 10.310 | 0.270 |
| ZN 78 | 2.258 | 1.032 | 6.010 | 1.600 | BR 91 | 3.417 | 2.139 | 9.180 | 0.542 |
| GA 78 | 2.901 | 2.161 | 8.140 | 5.090 | KR 91 | 2.055 | 1.617 | 6.200 | 8.570 |
| ZN 79 | 3.016 | 2.917 | 8.660 | 1.000 | RB 91 | 1.476 | 2.296 | 5.700 | 58.200 |
| GA 79 | 2.613 | 1.062 | 6.760 | 3.000 | BR 92 | 4.006 | 3.199 | 12.010 | 0.362 |
| GA 80 | 3.122 | 3.548 | 9.900 | 1.660 | KR 92 | 2.262 | 1.078 | 6.080 | 1.850 |
| GE 80 | 0.815 | 0.620 | 2.630 | 24.500 | RB 92 | 2.856 | 1.566 | 7.770 | 4.500 |
| AS 80 | 2.479 | 0.259 | 5.700 | 16.500 | KR 93 | 2.727 | 2.757 | 8.700 | 1.289 |
| GA 81 | 2.784 | 1.187 | 7.230 | 1.230 | RB 93 | 2.147 | 2.675 | 7.450 | 5.820 |
| GE 81 | 2.126 | 0.881 | 5.600 | 10.100 | KR 94 | 2.947 | 1.480 | 7.500 | 0.208 |
| GA 82 | 3.796 | 4.131 | 12.300 | 0.600 | RB 94 | 2.994 | 3.655 | 10.140 | 2.760 |
| GE 82 | 1.449 | 0.765 | 4.400 | 4.600 | KR 95 | 3.055 | 3.355 | 10.000 | 0.780 |
| AS 82 | 1.990 | 2.954 | 7.400 | 21.000 | RB 95 | 3.102 | 1.887 | 8.590 | 0.384 |
| AS 82M | 1.954 | 2.763 | 7.400 | 13.000 | SR 95 | 1.593 | 2.442 | 6.090 | 24.400 |
| GA 83 | 3.881 | 3.743 | 11.000 | 0.310 | RB 96 | 3.821 | 3.084 | 10.300 | 0.203 |
| GE 83 | 2.689 | 2.444 | 7.400 | 1.900 | SR 96 | 1.962 | 0.959 | 5.360 | 1.015 |
| AS 83 | 2.000 | 0.993 | 5.314 | 14.100 | SR 97 | 2.603 | 1.501 | 7.200 | 0.441 |
| GE 84 | 2.546 | 2.460 | 6.700 | 1.200 | Y 97 | 2.472 | 1.231 | 6.670 | 3.700 |
| AS 84 | 2.834 | 3.405 | 9.780 | 5.800 | Y 97M | 2.683 | 1.472 | 7.173 | 1.130 |
| AS 85 | 2.836 | 3.005 | 9.100 | 2.080 | RB 98 | 3.711 | 2.923 | 10.850 | 0.108 |
| SE 85 | 1.630 | 2.388 | 6.100 | 32.800 | SR 98 | 2.139 | 1.051 | 5.810 | 0.660 |
| AS 86 | 3.317 | 3.778 | 10.180 | 0.900 | Y 98 | 3.216 | 2.041 | 8.980 | 0.650 |
| SE 86 | 1.350 | 1.964 | 5.100 | 16.700 | Y 98M | 2.989 | 2.596 | 9.080 | 2.000 |
| BR 86 | 1.947 | 2.936 | 7.300 | 55.700 | RB 99 | 3.664 | 2.656 | 10.000 | 0.067 |
| AS 87 | 3.440 | 3.473 | 10.410 | 0.730 | SR 99 | 3.041 | 2.106 | 8.000 | 0.600 |
| SE 87 | 2.079 | 2.644 | 7.270 | 5.600 | Y 99 | 2.375 | 1.147 | 6.390 | 1.400 |
| BR 87 | 1.813 | 2.410 | 6.500 | 55.600 | NB100N | 1.564 | 2.831 | 6.430 | 168.000 |
| SE 88 | 2.404 | 1.716 | 7.000 | 1.530 | ZR101 | 2.160 | 1.091 | 5.900 | 2.400 |

Table II (cont'd)

| NUCLIDE | E-BETA (MEV) | E-GAMMA (MEV) | Q-VALUE (MEV) | HALF-LIFE (SEC) | NUCLIDE | E-BETA (MEV) | E-GAMMA (MEV) | Q-VALUE (MEV) | HALF-LIFE (SEC) |
|---|---|---|---|---|---|---|---|---|---|
| NB101 | 1.686 | 0.720 | 4.570 | 7.300 | AG116M | 2.313 | 1.043 | 6.059 | 10.400 |
| Y 102 | 3.096 | 3.823 | 9.000 | 0.900 | RH117 | 2.289 | 1.359 | 7.350 | 1.700 |
| ZR102 | 1.250 | 0.737 | 4.000 | 2.900 | PD117 | 1.915 | 1.087 | 5.700 | 5.000 |
| NB102 | 2.832 | 1.461 | 7.200 | 1.300 | PD118 | 1.044 | 0.715 | 4.000 | 3.100 |
| NB102M | 2.832 | 1.461 | 7.200 | 4.300 | AG118 | 2.515 | 1.434 | 7.000 | 3.760 |
| NB103 | 2.111 | 0.982 | 5.200 | 1.500 | AG118M | 0.789 | 0.552 | 2.298 | 2.000 |
| MO103 | 1.144 | 1.134 | 4.300 | 67.500 | AG122 | 3.048 | 2.511 | 9.170 | 0.480 |
| ZR104 | 1.742 | 0.894 | 5.150 | 1.000 | IN122 | 2.363 | 1.242 | 6.510 | 1.500 |
| NB104M | 3.125 | 2.134 | 8.850 | 0.800 | IN122M | 2.423 | 1.499 | 6.590 | 10.000 |
| NB104 | 2.510 | 3.376 | 8.800 | 4.800 | AG123 | 2.640 | 1.859 | 7.000 | 0.390 |
| MO104 | 0.623 | 0.585 | 2.200 | 59.400 | CD123 | 1.866 | 1.099 | 5.500 | 5.000 |
| TC104 | 1.244 | 2.678 | 5.620 | 1092.000 | IN124 | 2.510 | 1.570 | 7.140 | 3.210 |
| NB105 | 2.499 | 1.404 | 6.940 | 3.000 | IN124M | 2.558 | 1.661 | 7.330 | 2.400 |
| MO105 | 1.290 | 2.365 | 5.400 | 36.700 | IN125 | 1.937 | 1.080 | 5.455 | 2.320 |
| NB106 | 3.313 | 2.549 | 9.900 | 1.000 | IN125M | 1.660 | 1.836 | 5.632 | 12.200 |
| MO106 | 1.232 | 0.746 | 3.340 | 8.400 | IN126 | 2.735 | 2.026 | 8.060 | 1.530 |
| TC106 | 1.697 | 2.933 | 6.300 | 36.000 | IN126M | 2.774 | 2.097 | 8.210 | 2.100 |
| MO107 | 2.317 | 1.393 | 6.200 | 3.500 | IN127 | 2.252 | 1.443 | 6.486 | 1.300 |
| TC107 | 1.682 | 0.986 | 4.200 | 21.000 | IN127M | 2.191 | 1.727 | 6.615 | 3.760 |
| TC108 | 2.249 | 2.993 | 8.000 | 5.000 | CD128 | 1.831 | 1.003 | 5.280 | 0.940 |
| TC109 | 2.144 | 1.099 | 6.300 | 1.400 | IN128 | 3.049 | 2.633 | 9.310 | 0.840 |
| TC110 | 3.032 | 2.170 | 8.000 | 1.000 | IN128M | 2.634 | 3.557 | 9.390 | 5.600 |
| RU110 | 0.659 | 0.597 | 2.500 | 15.900 | IN129 | 2.588 | 1.861 | 7.322 | 0.990 |
| RH110 | 2.202 | 0.486 | 5.400 | 3.000 | IN129M | 2.155 | 2.947 | 7.410 | 2.500 |
| RH110M | 2.237 | 0.777 | 5.450 | 28.500 | IN130 | 3.063 | 2.693 | 9.400 | 0.576 |
| RU111 | 1.867 | 0.962 | 5.600 | 3.000 | IN131 | 2.707 | 2.017 | 7.132 | 0.270 |
| RH111 | 1.459 | 0.720 | 3.500 | 63.000 | SN131M | 1.098 | 2.391 | 5.050 | 61.000 |
| RU112 | 1.114 | 0.725 | 3.600 | 0.690 | IN132 | 3.158 | 2.898 | 9.800 | 0.130 |
| RH112 | 2.477 | 1.156 | 7.200 | 4.650 | SB132 | 1.197 | 2.728 | 5.600 | 168.000 |
| RU113 | 2.249 | 1.416 | 6.700 | 3.000 | SN133 | 2.410 | 1.861 | 7.240 | 1.470 |
| RH113 | 1.733 | 0.816 | 5.200 | 0.900 | SN134 | 2.295 | 1.248 | 6.070 | 1.040 |
| RH114 | 2.742 | 1.753 | 8.300 | 1.680 | SB134 | 2.781 | 2.256 | 8.400 | 0.850 |
| PD115 | 1.435 | 1.067 | 4.486 | 37.400 | SB134M | 2.284 | 3.272 | 8.892 | 10.400 |
| RH116 | 2.967 | 2.220 | 9.000 | 2.000 | SB135 | 2.480 | 1.790 | 7.520 | 1.710 |
| PD116 | 0.662 | 0.604 | 2.500 | 13.600 | TE135 | 1.532 | 2.620 | 6.200 | 19.200 |
| AG116 | 1.397 | 2.825 | 6.100 | 160.800 | SB136 | 2.953 | 2.605 | 9.540 | 0.820 |

Table II (cont'd)

| NUCLIDE | E-BETA (MEV) | E-GAMMA (MEV) | Q-VALUE (MEV) | HALF-LIFE (SEC) |
|---|---|---|---|---|
| I 136 | 1.760 | 2.942 | 7.000 | 85.100 |
| I 136M | 1.760 | 2.942 | 7.010 | 44.800 |
| TE137 | 2.173 | 1.609 | 6.480 | 2.800 |
| I 137 | 1.272 | 2.460 | 5.500 | 24.500 |
| TE138 | 1.946 | 1.068 | 5.340 | 1.400 |
| CS138 | 1.089 | 2.680 | 5.340 | 1932.000 |
| CS138M | 0.280 | 0.734 | 1.415 | 174.000 |
| I 139 | 2.059 | 1.324 | 6.000 | 2.380 |
| XE139 | 1.002 | 2.239 | 5.020 | 39.500 |
| I 140 | 2.762 | 2.328 | 8.930 | 0.600 |
| CS140 | 1.429 | 2.791 | 6.170 | 63.700 |
| I 141 | 2.425 | 1.779 | 7.420 | 0.470 |
| XE141 | 2.048 | 1.489 | 6.150 | 1.730 |
| CS141 | 1.276 | 2.135 | 5.190 | 24.900 |
| XE142 | 1.758 | 0.977 | 5.040 | 1.240 |
| CS142 | 2.449 | 1.787 | 7.280 | 1.710 |
| XE143 | 2.225 | 1.727 | 6.650 | 0.300 |
| CS143 | 1.935 | 1.217 | 5.650 | 1.780 |
| XE144M | 1.345 | 1.470 | 4.670 | 8.800 |
| XE144 | 1.606 | 0.923 | 4.670 | 1.150 |
| CS144 | 2.649 | 2.193 | 8.100 | 1.002 |
| BA144 | 0.946 | 0.705 | 2.900 | 11.850 |
| LA144 | 1.338 | 2.091 | 5.500 | 42.100 |
| XE145 | 2.291 | 1.827 | 6.300 | 0.900 |
| CS145 | 2.070 | 1.387 | 6.100 | 0.585 |
| BA145 | 1.757 | 1.159 | 5.100 | 3.790 |
| LA145 | 1.452 | 0.802 | 4.200 | 25.300 |
| CS146 | 2.632 | 2.190 | 8.540 | 0.335 |
| BA146 | 1.159 | 0.774 | 3.900 | 2.180 |
| LA146 | 2.182 | 1.345 | 6.300 | 8.500 |
| CS147 | 2.219 | 1.581 | 7.200 | 0.218 |
| BA147 | 1.858 | 1.301 | 5.520 | 0.700 |
| LA147 | 1.632 | 0.936 | 4.750 | 4.430 |
| BA148 | 1.343 | 0.835 | 4.040 | 0.470 |
| LA148 | 2.175 | 1.361 | 7.050 | 1.290 |
| PR150 | 2.017 | 1.074 | 5.700 | 6.200 |
| CE151 | 1.440 | 0.877 | 4.760 | 1.020 |
| PR151 | 1.234 | 0.701 | 3.500 | 4.000 |
| PM152N | 1.054 | 0.965 | 3.720 | 1080.000 |
| ND154 | 0.517 | 0.585 | 2.000 | 40.000 |

Note) Half-lives given in this table are measured values. The key parameter $Q_{00}$ was searched for and fixed so as that the gross theory calcution should reproduce these half-lives in the best way for individual nuclides (see text). Average energies were calculated on the basis of these $Q_{00}$ values.

Table III　Average β-and γ-ray Energies for $t_{1/2}$-unknown Nuclides (Gross Theory)

| NUCLIDE | E-BETA (MEV) | E-GAMMA (MEV) | Q-VALUE (MEV) | HALF-LIFE* (SEC) | NUCLIDE | E-BETA (MEV) | E-GAMMA (MEV) | Q-VALUE (MEV) | HALF-LIFE* (SEC) |
|---|---|---|---|---|---|---|---|---|---|
| CR 66 | 3.863 | 1.693 | 9.878 | 0.267 | CO 74 | 5.167 | 5.420 | 16.220 | 0.082 |
| MN 66 | 4.739 | 4.644 | 14.580 | 0.175 | NI 74 | 2.683 | 1.199 | 7.029 | 1.437 |
| FE 66 | 2.267 | 1.047 | 6.036 | 3.666 | CU 74 | 2.511 | 3.206 | 8.697 | 4.985 |
| CO 66 | 2.905 | 3.373 | 9.653 | 2.785 | CO 75 | 5.259 | 3.745 | 14.730 | 0.065 |
| CR 67 | 4.932 | 3.137 | 13.450 | 0.113 | NI 75 | 3.827 | 2.216 | 10.340 | 0.451 |
| MN 67 | 4.531 | 2.453 | 11.970 | 0.216 | CU 75 | 2.688 | 1.090 | 6.936 | 3.958 |
| FE 67 | 3.708 | 1.852 | 9.731 | 0.702 | FE 76 | 5.133 | 2.716 | 13.450 | 0.049 |
| CO 67 | 3.055 | 1.249 | 7.828 | 2.286 | CO 76 | 5.866 | 6.371 | 18.570 | 0.036 |
| CR 68 | 4.391 | 2.009 | 11.250 | 0.131 | NI 76 | 3.379 | 1.527 | 8.752 | 0.439 |
| MN 68 | 5.072 | 5.050 | 15.650 | 0.109 | CU 76 | 3.113 | 3.504 | 10.200 | 1.574 |
| FE 68 | 2.729 | 1.215 | 7.133 | 1.469 | NI 77 | 4.481 | 3.088 | 12.520 | 0.153 |
| CO 68 | 3.685 | 3.809 | 11.650 | 0.739 | CU 77 | 3.267 | 1.506 | 8.512 | 1.260 |
| NI 68 | 0.664 | 0.582 | 2.256 | 576.100 | NI 78 | 3.929 | 1.877 | 10.200 | 0.194 |
| MN 69 | 4.984 | 3.070 | 13.490 | 0.109 | CU 78 | 3.830 | 4.053 | 12.180 | 0.464 |
| FE 69 | 4.046 | 2.236 | 10.790 | 0.381 | CU 79 | 3.709 | 1.970 | 9.858 | 0.549 |
| CO 69 | 3.561 | 1.613 | 9.203 | 0.909 | NI 80 | 5.305 | 2.961 | 14.050 | 0.039 |
| NI 69 | 2.327 | 0.933 | 6.051 | 9.290 | CU 80 | 4.327 | 4.587 | 13.710 | 0.213 |
| CR 70 | 5.084 | 2.532 | 13.150 | 0.057 | ZN 80 | 2.758 | 1.242 | 7.227 | 1.126 |
| MN 70 | 5.445 | 5.565 | 16.910 | 0.066 | CU 81 | 4.826 | 3.457 | 13.580 | 0.095 |
| FE 70 | 3.320 | 1.460 | 8.564 | 0.537 | ZN 81 | 4.032 | 2.713 | 11.250 | 0.267 |
| CO 70 | 4.154 | 4.208 | 12.980 | 0.348 | NI 82 | 5.983 | 3.536 | 15.990 | 0.020 |
| NI 70 | 1.240 | 0.713 | 3.607 | 49.230 | CU 82 | 4.689 | 5.062 | 14.910 | 0.125 |
| MN 71 | 5.574 | 3.910 | 15.520 | 0.050 | ZN 82 | 4.234 | 2.181 | 11.130 | 0.122 |
| FE 71 | 4.401 | 2.710 | 11.970 | 0.207 | ZN 83 | 4.102 | 3.953 | 12.630 | 0.160 |
| CO 71 | 4.102 | 2.162 | 10.830 | 0.360 | ZN 84 | 4.623 | 3.297 | 13.030 | 0.063 |
| NI 71 | 2.822 | 1.244 | 7.356 | 3.206 | GA 84 | 4.228 | 4.633 | 13.570 | 0.222 |
| CU 71 | 1.373 | 0.637 | 3.812 | 81.710 | GA 85 | 4.509 | 4.305 | 13.810 | 0.097 |
| FE 72 | 4.061 | 1.874 | 10.460 | 0.183 | GE 85 | 3.029 | 3.183 | 9.718 | 0.776 |
| CO 72 | 4.608 | 4.694 | 14.370 | 0.177 | ZN 86 | 5.261 | 3.685 | 14.700 | 0.033 |
| NI 72 | 1.882 | 0.913 | 5.126 | 7.843 | GA 86 | 4.647 | 5.172 | 14.950 | 0.120 |
| CU 72 | 2.035 | 2.994 | 7.521 | 14.790 | GE 86 | 3.362 | 2.636 | 9.843 | 0.283 |
| FE 73 | 4.903 | 3.407 | 13.670 | 0.097 | GE 87 | 3.533 | 3.585 | 11.130 | 0.327 |
| CO 73 | 4.718 | 2.980 | 12.880 | 0.137 | GE 88 | 4.006 | 3.003 | 11.500 | 0.119 |
| NI 73 | 3.281 | 1.619 | 8.650 | 1.262 | AS 88 | 3.752 | 4.221 | 12.210 | 0.412 |
| CU 73 | 1.985 | 0.772 | 5.201 | 17.830 | AS 89 | 3.977 | 3.943 | 12.390 | 0.177 |
| FE 74 | 4.670 | 2.324 | 12.130 | 0.084 | SE 92 | 4.113 | 2.237 | 10.970 | 0.123 |

*) Gross theory calculated value

Table III (cont'd)

| NUCLIDE | E-BETA (MEV) | E-GAMMA (MEV) | Q-VALUE (MEV) | HALF-LIFE (SEC) | NUCLIDE | E-BETA (MEV) | E-GAMMA (MEV) | Q-VALUE (MEV) | HALF-LIFE (SEC) |
|---|---|---|---|---|---|---|---|---|---|
| SE 93 | 4.117 | 4.142 | 12.880 | 0.132 | NB109 | 3.158 | 2.263 | 9.106 | 0.701 |
| BR 93 | 3.554 | 3.672 | 11.280 | 0.298 | MO109 | 2.675 | 1.876 | 7.743 | 1.722 |
| SE 94 | 4.189 | 2.300 | 11.180 | 0.109 | ZR110 | 2.844 | 1.509 | 7.713 | 0.605 |
| BR 94 | 4.019 | 4.661 | 13.200 | 0.244 | NB110 | 3.927 | 3.745 | 12.140 | 0.323 |
| SE 95 | 4.559 | 4.497 | 14.120 | 0.076 | MO110 | 2.199 | 1.152 | 6.056 | 2.018 |
| BR 95 | 3.593 | 3.713 | 11.400 | 0.272 | NB111 | 3.399 | 2.568 | 9.900 | 0.439 |
| SE 96 | 4.612 | 2.618 | 12.350 | 0.065 | MO111 | 3.098 | 2.413 | 9.142 | 0.690 |
| BR 96 | 4.469 | 4.822 | 14.270 | 0.142 | TC111 | 2.486 | 1.501 | 6.988 | 2.841 |
| KR 96 | 3.073 | 1.566 | 8.209 | 0.497 | NB112 | 4.178 | 4.186 | 13.100 | 0.204 |
| KR 97 | 3.834 | 2.993 | 11.170 | 0.249 | MO112 | 2.552 | 1.354 | 6.976 | 0.990 |
| KR 98 | 3.492 | 1.851 | 9.341 | 0.257 | TC112 | 3.340 | 2.790 | 10.010 | 0.985 |
| KR 99 | 4.299 | 3.531 | 12.650 | 0.124 | MO113 | 3.430 | 2.802 | 10.210 | 0.371 |
| KR100 | 3.970 | 2.189 | 10.640 | 0.133 | TC113 | 2.732 | 1.822 | 7.812 | 1.562 |
| RB100 | 4.276 | 4.674 | 13.750 | 0.175 | MO114 | 2.925 | 1.578 | 7.959 | 0.508 |
| SR100 | 2.531 | 1.275 | 6.832 | 1.197 | TC114 | 3.578 | 3.257 | 10.960 | 0.577 |
| RB101 | 4.038 | 3.123 | 11.720 | 0.187 | RU114 | 1.473 | 0.844 | 4.265 | 11.180 |
| SR101 | 3.466 | 2.662 | 10.110 | 0.421 | MO115 | 3.598 | 2.998 | 10.740 | 0.273 |
| Y 101 | 2.691 | 1.523 | 7.405 | 2.181 | TC115 | 2.995 | 2.162 | 8.687 | 0.872 |
| SR102 | 3.017 | 1.578 | 8.120 | 0.501 | RU115 | 2.538 | 1.806 | 7.407 | 2.120 |
| RB103 | 4.362 | 3.502 | 12.750 | 0.116 | RH115 | 2.021 | 1.054 | 5.605 | 8.607 |
| SR103 | 3.694 | 2.949 | 10.860 | 0.280 | MO116 | 3.178 | 1.737 | 8.632 | 0.334 |
| Y 103 | 3.034 | 1.981 | 8.558 | 1.005 | TC116 | 3.693 | 3.495 | 11.440 | 0.443 |
| ZR103 | 2.457 | 1.467 | 6.879 | 3.300 | RU116 | 1.843 | 0.986 | 5.170 | 4.181 |
| SR104 | 3.430 | 1.852 | 9.229 | 0.262 | TC117 | 3.173 | 2.390 | 9.278 | 0.600 |
| Y 104 | 3.494 | 3.750 | 11.260 | 0.565 | RU117 | 2.697 | 2.026 | 7.952 | 1.422 |
| SR105 | 4.083 | 3.388 | 12.080 | 0.152 | TC118 | 3.877 | 3.835 | 12.150 | 0.305 |
| Y 105 | 3.325 | 2.372 | 9.539 | 0.554 | RU118 | 2.094 | 1.118 | 5.817 | 2.305 |
| ZR105 | 2.662 | 1.764 | 7.593 | 1.931 | RH118 | 3.094 | 2.494 | 9.230 | 1.520 |
| Y 106 | 3.813 | 4.187 | 12.340 | 0.320 | RU119 | 2.920 | 2.311 | 8.693 | 0.859 |
| ZR106 | 2.138 | 1.091 | 5.859 | 2.429 | RH119 | 2.476 | 1.598 | 7.078 | 2.547 |
| Y 107 | 3.667 | 2.801 | 10.660 | 0.299 | PD119 | 2.111 | 1.337 | 6.077 | 5.957 |
| ZR107 | 2.982 | 2.201 | 8.680 | 0.926 | RU120 | 2.361 | 1.266 | 6.512 | 1.301 |
| NB107 | 2.815 | 1.816 | 7.962 | 1.454 | RH120 | 3.261 | 2.837 | 9.914 | 0.999 |
| ZR108 | 2.567 | 1.339 | 6.980 | 1.007 | PD120 | 1.343 | 0.814 | 3.973 | 15.240 |
| NB108 | 3.587 | 3.108 | 10.820 | 0.641 | RH121 | 2.671 | 1.852 | 7.731 | 1.573 |
| ZR109 | 3.387 | 2.703 | 10.000 | 0.420 | PD121 | 2.335 | 1.638 | 6.837 | 3.160 |

Table III (cont'd)

| NUCLIDE | E-BETA (MEV) | E-GAMMA (MEV) | Q-VALUE (MEV) | HALF-LIFE (SEC) | NUCLIDE | E-BETA (MEV) | E-GAMMA (MEV) | Q-VALUE (MEV) | HALF-LIFE (SEC) |
|---|---|---|---|---|---|---|---|---|---|
| RU122 | 2.680 | 1.450 | 7.346 | 0.707 | TE142 | 2.513 | 1.375 | 6.986 | 0.773 |
| RH122 | 3.370 | 3.070 | 10.370 | 0.758 | I 142 | 2.692 | 3.203 | 9.186 | 1.561 |
| PD122 | 1.650 | 0.921 | 4.718 | 6.307 | XE146 | 1.971 | 1.086 | 5.592 | 2.239 |
| RH123 | 2.903 | 2.147 | 8.499 | 0.930 | XE148 | 2.553 | 1.402 | 7.112 | 0.668 |
| PD123 | 2.495 | 1.859 | 7.385 | 2.055 | CS148 | 2.454 | 2.969 | 8.477 | 2.468 |
| RU124 | 3.067 | 1.684 | 8.370 | 0.364 | BA149 | 2.016 | 1.520 | 6.129 | 4.831 |
| RH124 | 3.496 | 3.326 | 10.880 | 0.562 | LA149 | 1.783 | 1.087 | 5.217 | 10.770 |
| PD124 | 1.981 | 1.072 | 5.551 | 2.776 | XE150 | 3.092 | 1.722 | 8.542 | 0.263 |
| AG124 | 3.090 | 2.622 | 9.366 | 1.369 | CS150 | 2.751 | 3.331 | 9.452 | 1.219 |
| PD125 | 2.671 | 2.092 | 7.980 | 1.324 | BA150 | 1.985 | 1.096 | 5.645 | 2.052 |
| AG125 | 2.591 | 1.815 | 7.545 | 1.767 | LA150 | 2.037 | 2.547 | 7.206 | 6.756 |
| CD125 | 2.061 | 1.348 | 5.997 | 6.244 | LA151 | 2.202 | 1.601 | 6.602 | 3.049 |
| PD126 | 2.359 | 1.276 | 6.529 | 1.231 | BA152 | 2.524 | 1.390 | 7.057 | 0.666 |
| AG126 | 2.996 | 3.438 | 9.994 | 1.031 | LA152 | 2.355 | 2.885 | 8.203 | 2.942 |
| AG127 | 2.887 | 2.181 | 8.517 | 0.903 | CE152 | 1.166 | 0.778 | 3.617 | 18.630 |
| CD127 | 2.073 | 2.001 | 6.677 | 4.101 | PR152 | 1.549 | 2.119 | 5.770 | 27.100 |
| PD128 | 2.761 | 1.506 | 7.581 | 0.579 | LA153 | 2.595 | 2.088 | 7.906 | 1.107 |
| AG128 | 3.199 | 3.699 | 10.670 | 0.675 | CE153 | 1.680 | 1.125 | 5.045 | 13.350 |
| CD129 | 2.304 | 2.228 | 7.377 | 2.258 | PR153 | 1.700 | 1.027 | 4.994 | 13.130 |
| PD130 | 3.893 | 2.211 | 10.600 | 0.108 | ND153 | 0.969 | 0.623 | 3.045 | 169.000 |
| AG130 | 4.300 | 5.022 | 14.240 | 0.110 | BA154 | 2.956 | 1.645 | 8.203 | 0.308 |
| CD130 | 2.258 | 1.225 | 6.284 | 1.447 | LA154 | 2.615 | 3.199 | 9.057 | 1.543 |
| CD131 | 3.518 | 3.267 | 10.900 | 0.230 | CE154 | 1.694 | 0.959 | 4.914 | 3.899 |
| CD132 | 3.405 | 1.897 | 9.305 | 0.203 | PR154 | 1.873 | 2.414 | 6.745 | 9.938 |
| IN134 | 3.992 | 4.699 | 13.310 | 0.162 | CE155 | 2.015 | 1.571 | 6.191 | 4.354 |
| SN135 | 2.555 | 2.482 | 8.162 | 1.196 | PR155 | 2.071 | 1.480 | 6.224 | 4.054 |
| CD136 | 4.098 | 2.351 | 11.170 | 0.078 | ND155 | 1.366 | 0.834 | 4.104 | 38.610 |
| IN136 | 4.383 | 5.157 | 14.570 | 0.090 | PM155 | 1.020 | 0.633 | 3.171 | 123.900 |
| SN136 | 2.614 | 1.427 | 7.233 | 0.687 | CE156 | 2.118 | 1.171 | 6.010 | 1.414 |
| SN137 | 2.970 | 2.831 | 9.363 | 0.525 | PR156 | 2.149 | 2.688 | 7.595 | 4.627 |
| SB137 | 2.573 | 2.389 | 8.114 | 1.213 | ND156 | 1.122 | 0.766 | 3.520 | 20.390 |
| SN138 | 3.011 | 1.661 | 8.279 | 0.345 | PM156 | 1.314 | 1.894 | 5.055 | 61.880 |
| SB138 | 3.030 | 3.578 | 10.240 | 0.813 | CE157 | 2.431 | 2.089 | 7.575 | 1.379 |
| SB139 | 2.908 | 2.684 | 9.096 | 0.613 | PR157 | 2.387 | 1.881 | 7.283 | 1.682 |
| TE139 | 2.376 | 2.351 | 7.678 | 1.661 | ND157 | 1.668 | 1.140 | 5.047 | 12.900 |
| TE140 | 2.336 | 1.275 | 6.522 | 1.108 | PM157 | 1.451 | 0.841 | 4.296 | 27.690 |

Table III (cont'd)

| NUCLIDE | E-BETA (MEV) | E-GAMMA (MEV) | Q-VALUE (MEV) | HALF-LIFE (SEC) | NUCLIDE | E-BETA (MEV) | E-GAMMA (MEV) | Q-VALUE (MEV) | HALF-LIFE (SEC) |
|---|---|---|---|---|---|---|---|---|---|
| CE158 | 2.608 | 1.445 | 7.301 | 0.527 | TB165 | 0.792 | 0.597 | 2.649 | 297.300 |
| PR158 | 2.552 | 3.155 | 8.900 | 1.660 | SM166 | 2.084 | 1.205 | 6.004 | 1.404 |
| ND158 | 1.589 | 0.924 | 4.669 | 4.818 | EU166 | 1.838 | 2.395 | 6.680 | 7.960 |
| PM158 | 1.569 | 2.164 | 5.869 | 23.270 | GD166 | 1.174 | 0.806 | 3.690 | 16.070 |
| SM158 | 0.408 | 0.555 | 1.716 | 768.800 | TB166 | 0.947 | 1.611 | 3.998 | 222.100 |
| PR159 | 2.773 | 2.338 | 8.542 | 0.674 | SM167 | 2.338 | 2.101 | 7.428 | 1.320 |
| ND159 | 2.063 | 1.666 | 6.401 | 3.477 | EU167 | 2.024 | 1.643 | 6.320 | 3.235 |
| PM159 | 1.782 | 1.160 | 5.312 | 9.107 | GD167 | 1.545 | 1.217 | 4.888 | 13.670 |
| SM159 | 1.127 | 0.689 | 3.461 | 88.120 | TB167 | 1.140 | 0.751 | 3.563 | 68.370 |
| CE160 | 2.931 | 1.700 | 8.226 | 0.312 | SM168 | 2.443 | 1.415 | 6.963 | 0.656 |
| PR160 | 2.639 | 3.233 | 9.159 | 1.142 | EU168 | 2.168 | 2.749 | 7.728 | 3.090 |
| ND160 | 2.100 | 1.206 | 6.022 | 1.478 | GD168 | 1.521 | 0.933 | 4.559 | 5.397 |
| PM160 | 1.969 | 2.500 | 7.046 | 6.012 | TB168 | 1.170 | 1.853 | 4.728 | 71.240 |
| SM160 | 0.847 | 0.690 | 2.853 | 63.240 | DY168 | 0.318 | 0.543 | 1.488 | 1703.001 |
| ND161 | 2.160 | 1.879 | 6.817 | 2.295 | EU169 | 2.277 | 1.935 | 7.143 | 1.602 |
| PM161 | 2.108 | 1.696 | 6.534 | 2.858 | GD169 | 1.913 | 1.664 | 6.115 | 3.865 |
| SM161 | 1.507 | 1.138 | 4.717 | 17.600 | TB169 | 1.355 | 0.927 | 4.201 | 28.820 |
| EU161 | 1.132 | 0.732 | 3.518 | 76.320 | DY169 | 0.865 | 0.632 | 2.850 | 225.100 |
| ND162 | 2.485 | 1.431 | 7.049 | 0.659 | SM170 | 2.692 | 1.568 | 7.635 | 0.405 |
| PM162 | 2.079 | 2.620 | 7.396 | 4.348 | EU170 | 2.165 | 2.753 | 7.723 | 3.054 |
| SM162 | 1.383 | 0.878 | 4.198 | 8.806 | GD170 | 1.914 | 1.116 | 5.574 | 1.930 |
| EU162 | 1.403 | 2.018 | 5.384 | 32.430 | TB170 | 1.494 | 2.107 | 5.677 | 21.500 |
| ND163 | 2.482 | 2.219 | 7.830 | 1.024 | DY170 | 0.646 | 0.628 | 2.356 | 147.200 |
| PM163 | 2.393 | 2.019 | 7.451 | 1.346 | GD171 | 1.988 | 1.760 | 6.369 | 3.023 |
| SM163 | 1.669 | 1.334 | 5.254 | 9.597 | TB171 | 1.594 | 1.168 | 4.950 | 11.780 |
| EU163 | 1.541 | 1.072 | 4.730 | 16.170 | DY171 | 1.250 | 0.929 | 3.981 | 40.120 |
| GD163 | 0.985 | 0.685 | 3.157 | 141.300 | HO171 | 0.713 | 0.581 | 2.464 | 403.500 |
| ND164 | 2.741 | 1.588 | 7.738 | 0.405 | GD172 | 2.199 | 1.279 | 6.335 | 1.001 |
| PM164 | 2.348 | 2.926 | 8.264 | 2.107 | TB172 | 1.511 | 2.125 | 5.732 | 19.930 |
| SM164 | 1.803 | 1.049 | 5.258 | 2.766 | DY172 | 1.014 | 0.753 | 3.300 | 26.300 |
| EU164 | 1.563 | 2.147 | 5.851 | 18.780 | HO172 | 0.944 | 1.645 | 4.034 | 197.400 |
| GD164 | 0.718 | 0.647 | 2.531 | 109.600 | | | | | |
| PM165 | 2.579 | 2.221 | 8.041 | 0.860 | | | | | |
| SM165 | 1.963 | 1.691 | 6.231 | 3.648 | | | | | |
| EU165 | 1.830 | 1.407 | 5.676 | 5.948 | | | | | |
| GD165 | 1.230 | 0.881 | 3.881 | 48.400 | | | | | |

Note) Half-lives are not measured for the nuclides given in this table. Calculated half-lives are listed here.

Table IV Average β-, γ-ray Energies and Related Parameters for 88 Nuclides with Experimental Information

| | $Q_\beta$ | $\overline{E}_\beta$ (MeV) | | | | $\overline{E}_\gamma$ (MeV) | | | | % contr. to $^{235}U$ decay heat | | Calculation Parameters | | |
|---|---|---|---|---|---|---|---|---|---|---|---|---|---|---|
| | (MeV) | JNDC(T) | JNDC(E) | ENDF/B-IV | ENDF/B-V | JNDC(T) | JNDC(E) | ENDF/B-IV | ENDF/B-V | tc= 20 sec | tc= 100 sec | $t_{1/2}$:input (sec) | $t_{1/2}$:calc'd (sec) | $Q_{00}$(MeV) |
| $Cu68^m$ | 5.341 | 0.20 | 0.19 | - | - | 0.96 | 0.98 | - | - | | | 225 | 208 | 2.0 |
| $Cu70^m$ | 6.310 | 1.65 | 1.58 | - | - | 2.17 | 2.93 | - | - | | | 46 | 46 | 1.7 |
| Cu70 | 6.170 | 2.70 | 2.57 | - | - | 0.30 | 0.58 | - | - | | | 4.5 | 16 | 0.0 |
| Ga74 | 5.400 | 1.29 | 1.02 | 1.07 | 1.99 | 2.40 | 3.05 | 3.04 | 0.95 | | | 495 | 182 | 2.0 |
| Ga76 | 6.770 | 1.75 | 1.81 | 1.68 | 1.92 | 2.50 | 2.79 | 2.81 | 2.79 | | | 271 | 272 | 1.8 |
| As80 | 5.700 | 2.48 | 2.32 | 2.52 | 2.46 | 0.26 | 0.61 | 0.61 | 0.61 | | | 16.5 | 22.3 | 0.0 |
| Ge81 | 5.600 | 2.13 | 2.49 | 2.06 | 2.27 | 0.88 | 0.12 | 1.19 | 0.51 | | | 10.1 | 12.3 | 0.5 |
| $As82^m$ | 7.417 | 1.95 | 1.86 | 1.82 | 1.81 | 2.76 | 3.16 | 2.99 | 3.10 | | | 13 | 12.9 | 1.9 |
| As82 | " | 1.99 | 3.25 | 3.21 | 3.16 | 2.95 | 0.48 | 0.29 | 0.40 | | | 21 | 13.4 | 2.0 |
| As83 | 5.460 | 2.00 | 1.26 | 1.68 | 1.83 | 0.99 | 2.75 | 0.98 | 1.31 | 0.4 | | 14.1 | 14.5 | 0.7 |
| As84 | 9.554 | 2.83 | 3.99 | 3.76 | 3.41 | 3.41 | 1.58 | 2.10 | 2.76 | | | 5.8 | 2.1 | 2.0 |
| Se85 | 6.100 | 1.63 | 1.70 | 2.06 | 2.18 | 2.39 | 2.24 | 1.29 | 1.40 | 0.9 | 0.9 | 32.8 | 18.1 | 2.0 |
| Se86 | 5.100 | 1.35 | 1.15 | 1.42 | 1.55 | 1.96 | 2.35 | 1.02 | 1.07 | 1.3 | | 16.7 | 16.1 | 1.8 |
| Br86 | 7.300 | 1.95 | 1.74 | 1.78 | 1.78 | 2.94 | 3.64 | 3.32 | 3.30 | 1.1 | 3.7 | 55.7 | 13.9 | 2.0 |
| Se87 | 7.270 | 2.08 | 2.49 | 2.50 | 2.54 | 2.64 | 1.96 | 1.74 | 1.71 | 0.5 | | 5.6 | 5.1 | 2.0 |
| Br87 | 6.500 | 1.81 | 1.54 | 2.14 | [illegible].49 | 2.41 | 3.86 | 1.73 | 1.55 | 1.6 | 3.4 | 55.6 | 11.0 | 2.0 |
| Se88 | 7.000 | 2.40 | 2.38 | 2.10 | 2.39 | 1.72 | 1.72 | 1.63 | 1.47 | | | 15.2 | 15.3 | 1.2 |
| Br88 | 8.600 | 2.45 | 2.62 | 3.07 | 2.54 | 3.21 | 3.06 | 1.88 | 3.00 | 3.1 | 0.6 | 16.3 | 41.4 | 2.0 |
| Rb88 | 5.309 | 1.19 | 2.09 | 2.08 | 2.06 | 2.49 | 0.64 | 0.67 | 0.66 | | | 1068 | 164 | 2.0 |
| Br90 | 10.330 | 3.09 | 4.39 | 3.36 | 3.21 | 3.66 | 1.13 | 2.32 | 2.62 | | | 1.96 | 1.18 | 2.0 |
| $Rb90^m$ | 6.467 | 1.54 | 1.29 | 1.11 | 1.36 | 2.67 | 3.35 | 3.62 | 3.10 | | 1.0 | 258 | 31.8 | 2.0 |
| Rb90 | 6.360 | 1.57 | 1.89 | 1.66 | 2.20 | 2.76 | 2.16 | 2.66 | 1.06 | 0.4 | 4.6 | 153 | 36.3 | 2.0 |
| Kr91 | 6.200 | 2.06 | 1.99 | 2.58 | 1.94 | 1.62 | 1.73 | 0.72 | 1.73 | 3.1 | | 8.57 | 8.48 | 1.1 |
| Rb91 | 5.700 | 1.48 | 1.52 | 1.33 | 1.50 | 2.30 | 2.22 | 2.73 | 2.26 | 2.8 | 7.0 | 58.2 | 26.3 | 2.0 |

Table IV (cont'd)

| | $Q_\beta$ | $\overline{E}_\beta$ (MeV) | | | | $\overline{E}_\gamma$ (MeV) | | | | % contr. to $^{235}U$ decay heat | | Calculation Parameters | | |
|---|---|---|---|---|---|---|---|---|---|---|---|---|---|---|
| | (MeV) | JNDC(T) | JNDC(E) | ENDF/B-IV | ENDF/B-V | JNDC(T) | JNDC(E) | ENDF/B-IV | ENDF/B-V | tc= 20 sec | tc= 100 sec | $t_{1/2}$:input (sec) | $t_{1/2}$:calc'd (sec) | $Q_{00}$(MeV) |
| Kr92 | 6.080 | 2.26 | 2.41 | 2.40 | 2.37 | 1.08 | 0.72 | 0.75 | 0.75 | | | 1.85 | 2.32 | 0.5 |
| Rb92 | 7.770 | 2.86 | 3.49 | 3.46 | 3.48 | 1.57 | 0.27 | 0.26 | 0.26 | 2.5 | | 4.5 | 4.54 | 0.3 |
| Kr93 | 8.700 | 2.73 | 2.89 | 2.76 | 2.34 | 2.76 | 2.28 | 2.04 | 2.24 | | | 1.29 | 1.29 | 1.6 |
| Rb93 | 7.450 | 2.15 | 2.72 | 2.03 | 2.61 | 2.68 | 1.39 | 1.41 | 1.32 | 2.6 | | 5.82 | 3.98 | 2.0 |
| Sr95 | 6.090 | 1.59 | 2.27 | 1.94 | 2.11 | 2.44 | 1.03 | 1.36 | 1.40 | 4.4 | 2.5 | 24.4 | 15.4 | 2.0 |
| Sr96 | 5.360 | 1.96 | 1.98 | 1.35 | 1.88 | 0.96 | 0.91 | 1.12 | 1.13 | | | 1.015 | 4.17 | 0.5 |
| Sr97 | 7.200 | 2.60 | 2.54 | 2.35 | 2.62 | 1.50 | 1.49 | 1.84 | 1.49 | | | 0.441 | 2.20 | 0.5 |
| $Y97^m$ | 7.338 | 2.68 | 2.40 | - | 2.42 | 1.47 | 1.80 | - | 1.82 | | | 1.13 | 2.38 | 0.5 |
| Y97 | 6.670 | 2.47 | 2.15 | 2.16 | 2.15 | 1.23 | 1.81 | 0.94 | 1.80 | 1.0 | | 3.7 | 3.75 | 0.4 |
| Rb98 | 10.850 | 3.71 | 3.81 | 3.64 | 4.15 | 2.92 | 1.25 | 3.16 | 4.68 | | | 0.108 | 0.646 | 0.0 |
| Sr98 | 5.810 | 2.14 | 2.53 | 1.69 | 2.53 | 1.05 | 0.17 | 1.50 | 0.18 | | | 0.66 | 2.73 | 0.5 |
| $Y98^m$ | 9.080 | 2.99 | 2.68 | - | 2.98 | 2.60 | 3.11 | - | 0.81 | | | 2.00 | 2.00 | 0.6 |
| Y98 | 8.980 | 3.22 | 3.95 | 2.84 | 1.81 | 2.04 | 0.81 | 1.94 | 3.15 | | | 0.65 | 1.87 | 0.0 |
| Y99 | 6.390 | 2.38 | 2.48 | 2.09 | 2.61 | 1.15 | 0.49 | 1.65 | 0.61 | | | 1.4 | 4.73 | 0.5 |
| Nb100 | 6.23 | 2.23 | 2.28 | 2.06 | 2.19 | 1.28 | 1.35 | 1.92 | 1.38 | 5.5 | | 1.5 | 16.1 | 0.5 |
| Zr101 | 5.900 | 2.16 | 2.50 | 2.40 | 2.21 | 1.09 | 0.35 | 3.53 | 1.53 | | | 2.4 | ~7.0 | 0.5 |
| TC104 | 5.620 | 1.24 | 1.68 | 1.19 | 1.58 | 2.68 | 1.84 | 1.15 | 1.94 | | | 1092 | 72.4 | 2.0 |
| Mo105 | 5.400 | 1.29 | 2.26 | 1.72 | 1.68 | 2.37 | 0.15 | 1.40 | 1.09 | 0.5 | 0.5 | 36.7 | 31.9 | 2.0 |
| Tc108 | 8.000 | 2.25 | 3.29 | 2.62 | 2.47 | 2.99 | 0.80 | 2.00 | 1.88 | | | 5.0 | 4.99 | 1.6 |
| $Rh110^m$ | 5.400 | 2.24 | 1.35 | 2.48 | 2.37 | 0.78 | 2.21 | 0.06 | 0.06 | | | 28.5 | 27.9 | 0.2 |
| Rh110 | 5.400 | 2.20 | 2.38 | 1.35 | 1.18 | 0.49 | 0.06 | 2.27 | 2.48 | | | 3.0 | 24.0 | 0.0 |
| $Ag116^m$ | 6.312 | 2.31 | 1.94 | 1.96 | 1.67 | 1.04 | 1.68 | 1.59 | 1.54 | | | 10.4 | 11.7 | 0.0 |
| Ag116 | 6.100 | 1.40 | 2.72 | 2.19 | 1.71 | 2.83 | 0.87 | 0.71 | 1.39 | | | 160.8 | 32.9 | 2.0 |
| $Ag118^m$ | 7.128 | 0.79 | 0.79 | 1.30 | 0.11 | 0.55 | 1.16 | 1.23 | 1.27 | | | 2.0 | 6.28 | 0.0 |
| Ag118 | 7.000 | 2.52 | 2.54 | 2.32 | 2.41 | 1.43 | 1.33 | 1.99 | 1.95 | | | 3.76 | 6.9 | 0.0 |

Table IV (cont'd)

| | $Q_\beta$ | $\overline{E}_\beta$ (MeV) | | | | $\overline{E}_\gamma$ (MeV) | | | | % contr. to $^{235}U$ decay heat | | Calculation Parameters | | |
|---|---|---|---|---|---|---|---|---|---|---|---|---|---|---|
| | (MeV) | JNDC(T) | JNDC(E) | ENDF/B-IV | ENDF/B-V | JNDC(T) | JNDC(E) | ENDF/B-IV | ENDF/B-V | tc= 20 sec | tc= 100 sec | $t_{1/2}$:input (sec) | $t_{1/2}$:calc'd (sec) | $Q_{00}$(MeV) |
| Ag122 | 9.170 | 3.05 | 3.70 | 2.97 | 2.94 | 2.51 | 1.12 | 2.91 | 2.93 | | | 0.48 | 1.57 | 0.0 |
| In122$^m$ | 6.590 | 2.42 | 1.92 | 2.17 | 2.29 | 1.50 | 1.73 | 1.93 | 1.15 | | | 10 | 9.9 | 0.1 |
| In122 | 6.510 | 2.36 | 2.74 | 2.09 | 2.14 | 1.24 | 1.26 | 1.86 | 1.59 | | | 1.5 | 10.1 | 0.0 |
| In124$^m$ | 7.350 | 2.56 | 2.23 | - | 2.36 | 1.66 | 2.27 | - | 1.95 | | | 2.4 | 5.40 | 0.0 |
| In124 | 7.140 | 2.51 | 2.33 | 2.26 | 2.29 | 1.57 | 1.87 | 2.20 | 1.94 | | | 3.21 | 6.20 | 0.0 |
| In125$^m$ | 5.660 | 1.66 | 2.45 | 1.59 | 2.11 | 1.84 | 0.13 | 1.76 | 0.58 | | | 12.2 | 11.9 | 1.2 |
| In125 | 5.480 | 1.94 | 1.81 | 1.53 | 1.93 | 1.08 | 1.29 | 1.70 | 0.96 | | | 2.32 | 9.44 | 0.5 |
| In126$^m$ | 8.210 | 2.77 | 3.47 | - | - | 2.10 | 0.66 | - | - | | | 2.1 | 2.89 | 0.0 |
| In126 | 8.060 | 2.74 | 2.47 | 2.54 | 2.58 | 2.03 | 2.53 | 2.59 | 2.29 | | | 1.53 | 3.19 | 0.0 |
| In127$^m$ | 6.650 | 2.19 | 2.79 | 1.96 | 2.24 | 1.73 | 0.43 | 2.29 | 0.95 | | | 3.76 | 3.81 | 0.8 |
| In127 | 6.490 | 2.25 | 2.18 | 1.87 | 2.15 | 1.44 | 1.52 | 2.19 | 1.65 | | | 1.3 | 3.92 | 0.5 |
| In128$^m$ | 9.390 | 2.63 | 2.49 | - | 2.86 | 3.56 | 3.96 | - | 2.92 | | | 5.6 | 1.65 | 2.0 |
| In128 | 9.310 | 3.05 | 3.36 | 2.80 | 3.12 | 2.63 | 3.16 | 3.06 | 2.13 | | | 0.84 | 1.40 | 0.0 |
| In129$^m$ | 7.800 | 2.16 | 3.29 | - | 2.49 | 2.95 | 0.20 | - | 2.07 | | | 2.5 | 2.14 | 2.0 |
| In129 | 7.600 | 2.59 | 2.46 | 2.07 | 2.86 | 1.86 | 1.81 | 2.55 | 1.10 | | | 0.99 | 1.67 | 0.5 |
| In130 | 9.400 | 3.06 | 3.13 | 2.89 | 3.04 | 2.69 | 2.24 | 3.43 | 3.34 | | | 0.576 | 1.03 | 0.0 |
| In131 | 8.000 | 2.71 | 2.29 | 2.35 | 2.76 | 2.02 | 1.94 | 3.07 | 2.47 | | | 0.29 | ~1 | 0.5 |
| Sn131$^m$ | 5.050 | 1.10 | 1.17 | 1.30 | 1.47 | 2.39 | 1.63 | 1.71 | 1.00 | | | 61.0 | 40.4 | 2.0 |
| In132 | 9.800 | 3.16 | 2.24 | 3.82 | 3.63 | 2.90 | 4.48 | 4.66 | 5.00 | | | 0.13 | 1.00 | 0.0 |
| Sb132 | 5.600 | 1.20 | 1.20 | 1.72 | 1.38 | 2.73 | 2.57 | 2.01 | 2.60 | 0.3 | 1.6 | 168 | 53.4 | 2.0 |
| Sn133 | 7.240 | 2.41 | 3.10 | 2.08 | 2.39 | 1.86 | 0.39 | 2.80 | 1.98 | | | 1.47 | | |
| Sb134$^m$ | 8.400 | 2.28 | 3.14 | 2.95 | 2.80 | 3.27 | 2.03 | 2.09 | 2.04 | 0.3 | | 1.04 | 2.45 | 0.0 |
| Sb134 | 8.400 | 2.78 | 3.84 | 3.95 | 3.78 | 2.26 | 0.00 | 0.00 | 0.00 | | | 0.85 | 2.45 | 0.0 |
| Te135 | 6.200 | 1.53 | 2.44 | 1.63 | 2.40 | 2.62 | 0.69 | 2.17 | 0.74 | 2.7 | 0.8 | 19.2 | 9.04 | 2.0 |
| I136$^m$ | 7.000 | 1.76 | 2.31 | 1.94 | 2.13 | 2.94 | 2.00 | 1.93 | 2.00 | 1.1 | 1.8 | 44.8 | 10.8 | 2.0 |

Table IV (cont'd)

| | $Q_\beta$ | $\overline{E}_\beta$ (MeV) | | | | $\overline{E}_\gamma$ (MeV) | | | | % contr. to $^{235}U$ decay heat | | Calculation Parameters | | |
|---|---|---|---|---|---|---|---|---|---|---|---|---|---|---|
| | (MeV) | JNDC(T) | JNDC(E) | ENDF/B-IV | ENDF/B-V | JNDC(T) | JNDC(E) | ENDF/B-IV | ENDF/B-V | tc= 20 sec | tc= 100 sec | $t_{1/2}$:input (sec) | $t_{1/2}$:calc'd (sec) | $Q_{00}$(MeV) |
| I136 | 7.000 | 1.76 | 2.54 | 1.81 | 1.97 | 2.94 | 2.47 | 2.21 | 2.38 | 1.2 | 4.8 | 85.1 | 10.8 | 2.0 |
| I137 | 5.500 | 1.27 | 1.97 | 1.51 | 2.29 | 2.46 | 0.75 | 2.03 | 0.97 | 2.2 | 1.2 | 24.5 | 21.0 | 2.0 |
| Cs138$^m$ | 5.420 | 0.28 | 0.40 | 1.15 | 0.39 | 0.73 | 0.53 | 2.60 | 0.54 | | | 174 | 66.3 | 2.0 |
| Cs138 | 5.340 | 1.09 | 1.25 | 1.26 | 1.20 | 2.68 | 2.33 | 2.33 | 2.36 | | | 1932 | 74.3 | 2.0 |
| Xc139 | 5.020 | 1.00 | 1.74 | 1.79 | 1.70 | 2.24 | 0.89 | 0.93 | 0.76 | 2.6 | 3.4 | 39.5 | 39.7 | 2.0 |
| Cs140 | 6.170 | 1.43 | 1.75 | 1.93 | 1.65 | 2.79 | 2.22 | 2.13 | 2.30 | 2.4 | 8.0 | 63.7 | 25.1 | 2.0 |
| Xe141 | 6.150 | 2.05 | 2.36 | 1.57 | 2.35 | 1.49 | 1.04 | 2.27 | 0.78 | | | 1.73 | 5.03 | 0.5 |
| Cs141 | 5.190 | 1.28 | 2.09 | 1.38 | 1.91 | 2.14 | 0.67 | 1.82 | 0.80 | 3.0 | 1.8 | 2.49 | 2.48 | 1.7 |
| Xe142 | 5.040 | 1.76 | 1.85 | 1.10 | 1.66 | 0.98 | 1.19 | 1.77 | 1.12 | | | 1.24 | 3.87 | 0.5 |
| Cs142 | 7.280 | 2.45 | 2.62 | 2.04 | 2.50 | 1.79 | 3.81 | 2.54 | 1.17 | | | 1.71 | 5.29 | 0.0 |
| La144 | 5.500 | 1.34 | 1.79 | 1.51 | 1.46 | 2.09 | 1.31 | 1.94 | 1.83 | 2.5 | 5.8 | 4.21 | 4.23 | 1.2 |
| La146 | 6.300 | 2.18 | 2.46 | 1.77 | 2.05 | 1.35 | 0.72 | 2.36 | 1.73 | 2.1 | | 8.5 | 11.4 | 0.0 |
| La148 | 6.300 | 2.18 | 2.74 | 1.93 | 2.21 | 1.36 | 0.88 | 2.67 | 2.04 | | | 0.47 | 11.3 | 0.0 |
| Pr150 | 5.700 | 2.02 | 2.31 | 1.35 | 1.84 | 1.08 | 0.26 | 1.86 | 1.48 | 0.4 | | 6.2 | 19.1 | 0.0 |

Table V Values of $\overline{E}_\gamma / Q_\beta$ for three assumed beta-strength functions

| | | $Q_\beta$ = 6 MeV | $Q_\beta$ = 8 MeV | $Q_\beta$ = 10 MeV |
|---|---|---|---|---|
| Present simple calc. | $S_\beta \propto E$ | 0.27 | 0.27 | 0.26 |
| | $S_\beta \propto e^{E/1.5}$ | 0.25 | 0.29 | 0.34 |
| | $S_\beta \propto e^{E}$ | 0.33 | 0.40 | 0.48 |
| Tasaka, Ref. 5) | | 0.29 | 0.29 | 0.29 |
| Tobias, Ref. 20) | | 0.33 | 0.33 | 0.33 |
| Yamamoto, Ref. 38) | | ~0.25 for light and ~0.35 for heavy peaks | | |

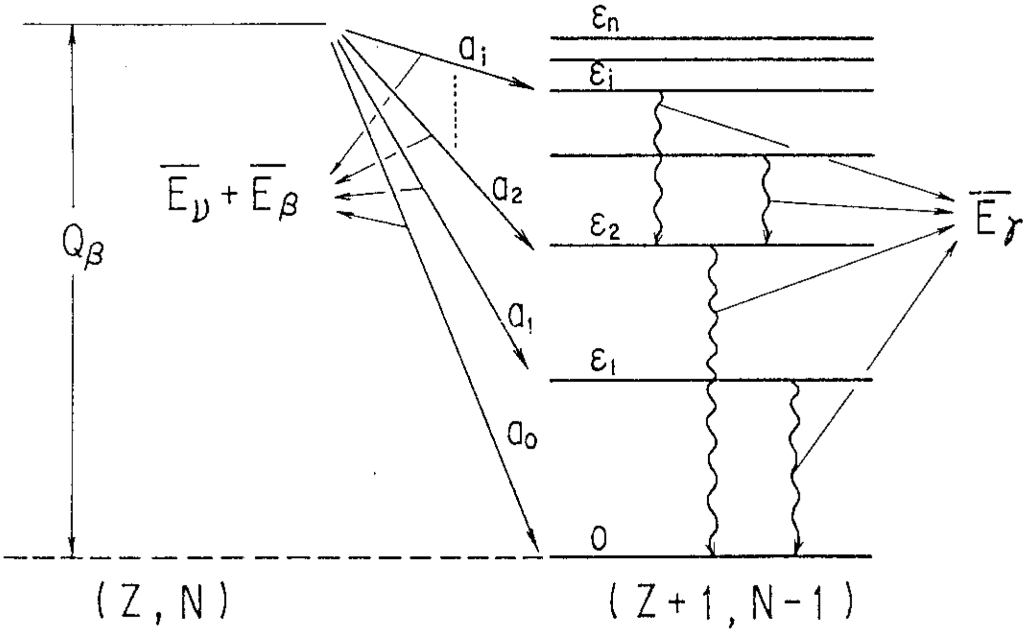


Fig. 1 Schematic display of beta- and gamma-decay process from a parent (Z, N) to the daughter (Z + 1, N - 1)

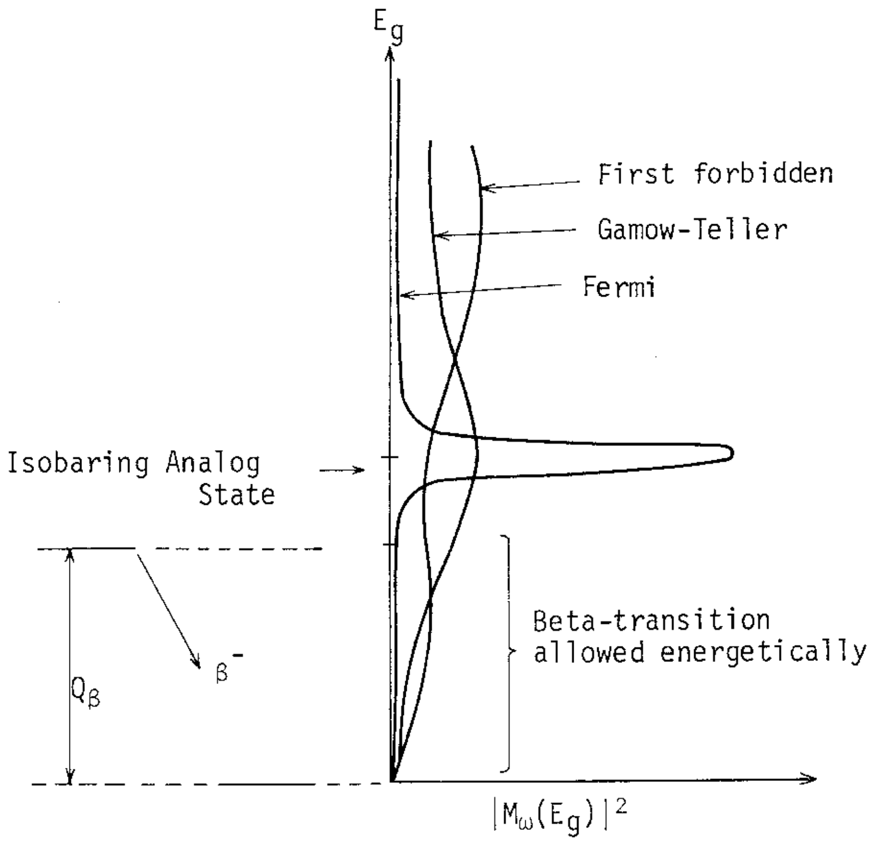


Fig. 2 Schematic view of beta-strength function

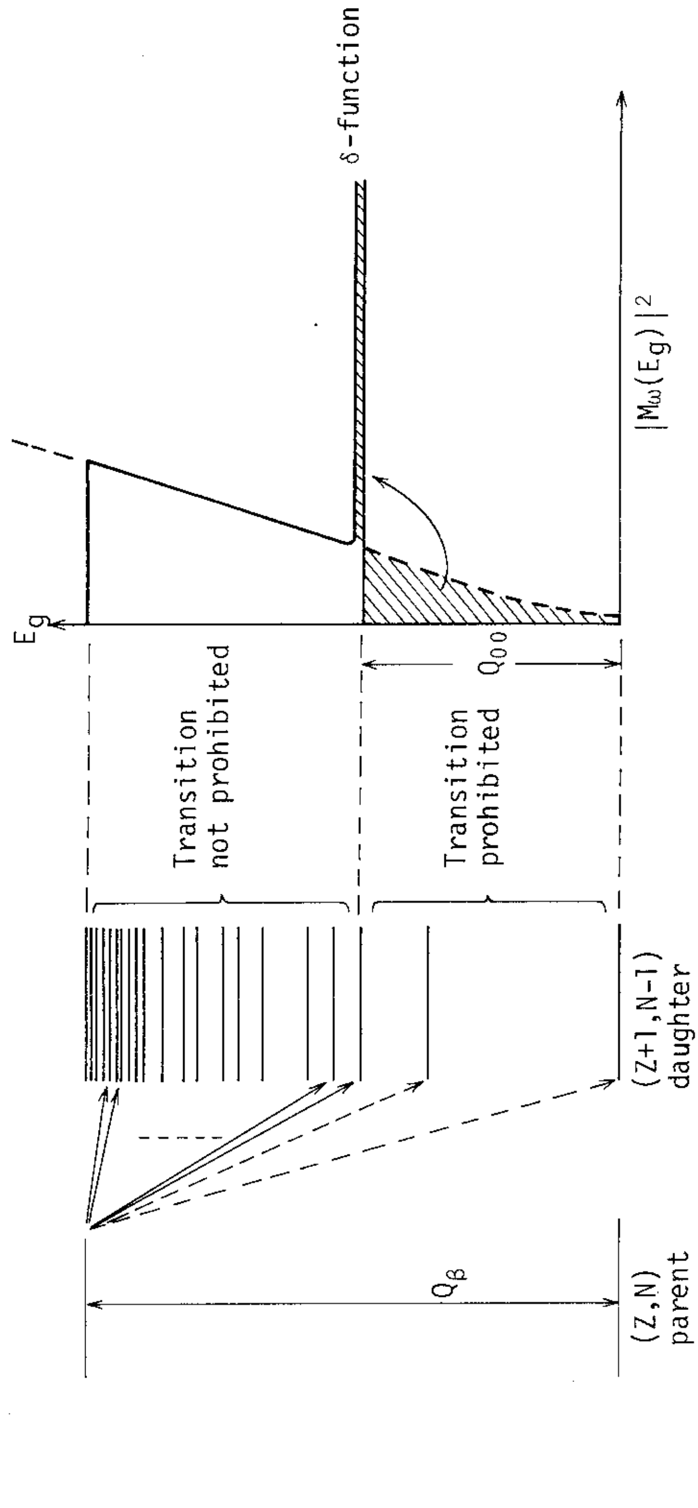


Fig. 3 Introduction of a parameter $Q_{00}$

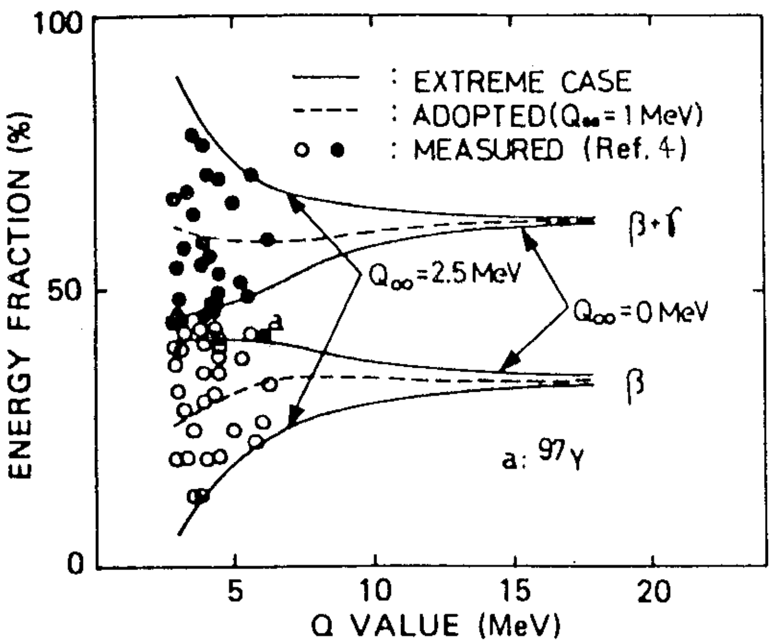


Fig. 4 Percentage of average beta-particle and gamma-ray energies from odd-$A$ fission products, and comparison of calculation with experiment (Ref. 4). (Total decay energy = 100%, calculated at $A$ = 89.)

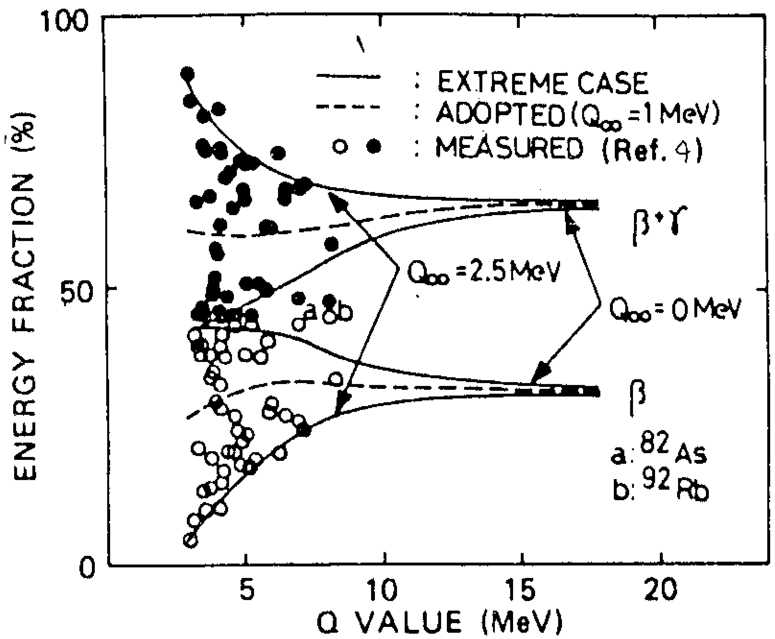


Fig. 5 Percentage of average beta-particle and gamma-ray energies from odd-odd fission products, and comparison of calculation with experiment (Ref. 4). (Total decay energy = 100%, calculated at $A$ = 90.)

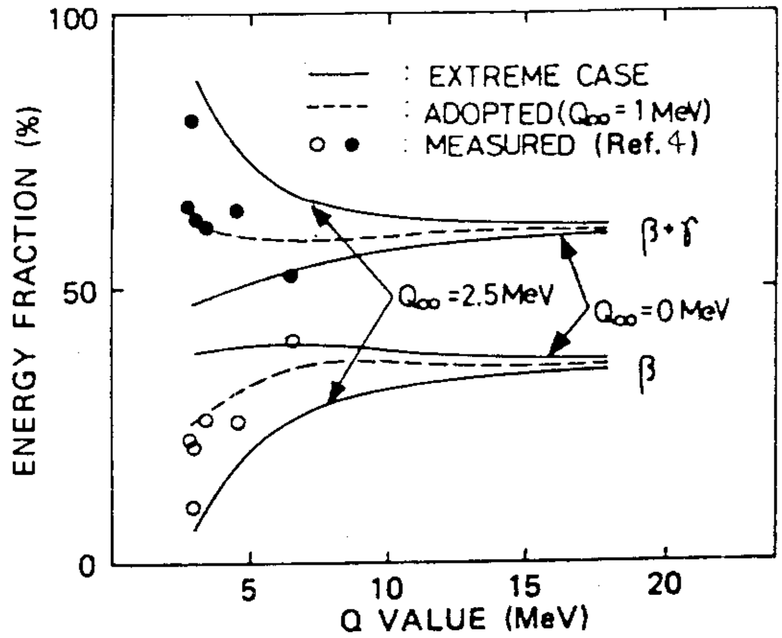


Fig.6 Percentage of average beta-particle and gamma-ray energies from even-even fission products, and comparison of calculation with experiment (Ref. 4). (Total decay energy = 100%, calculated at $A$ = 90.)

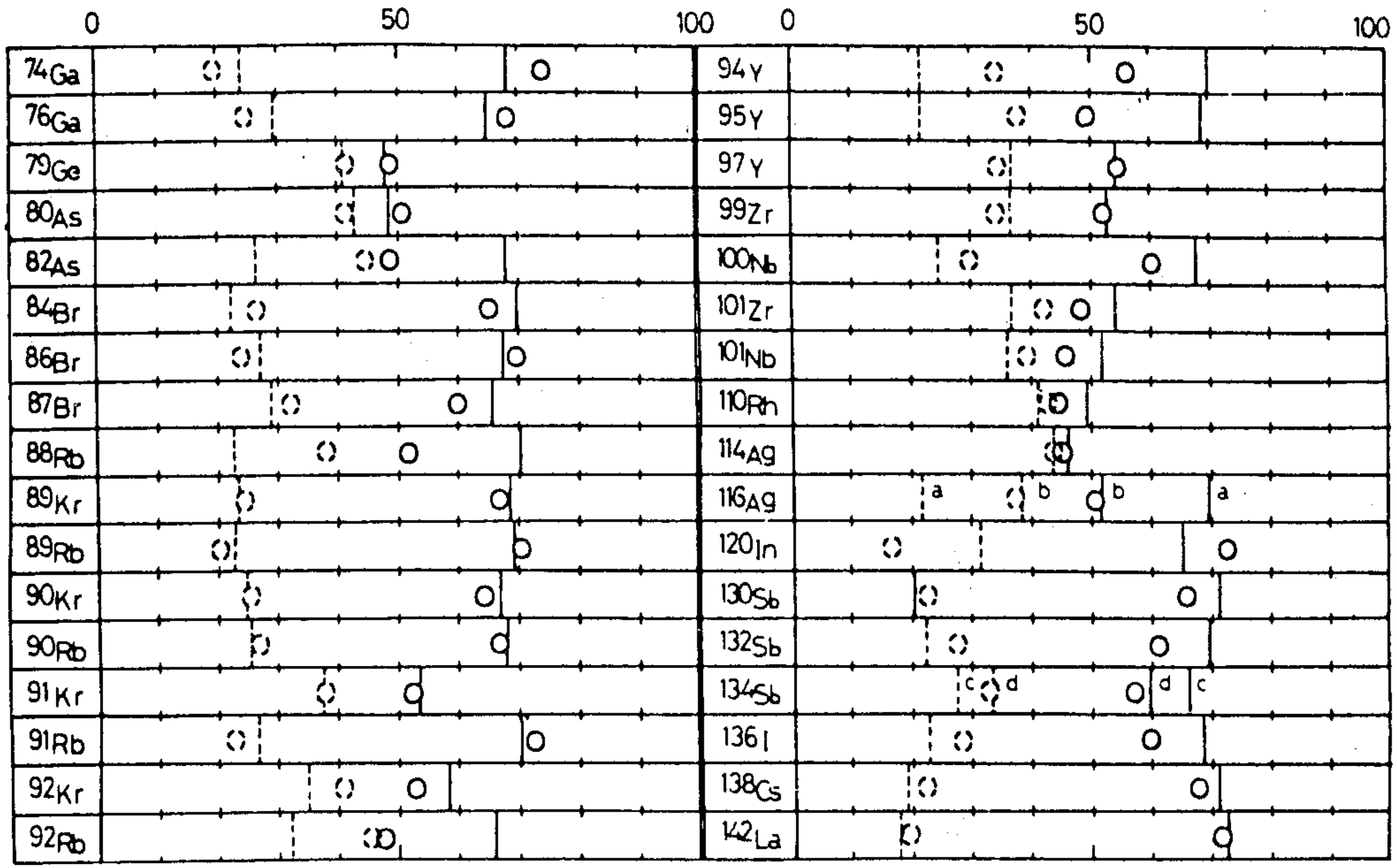


Fig.7 Percentage of average beta-particle and gamma-ray energies from fission products, with $Q_{00}$ determined from half-life data. Here, a dot = beta energy, a solid = beta-particle plus gamma-ray energy, a circle = experimental value (Refs. 4 and 2 ), and a line = calculated value. Lines a and c are based on $t_{1/2}$ from Ref. 4 and b and d from Ref. 39. (Total decay energy = 100%.)

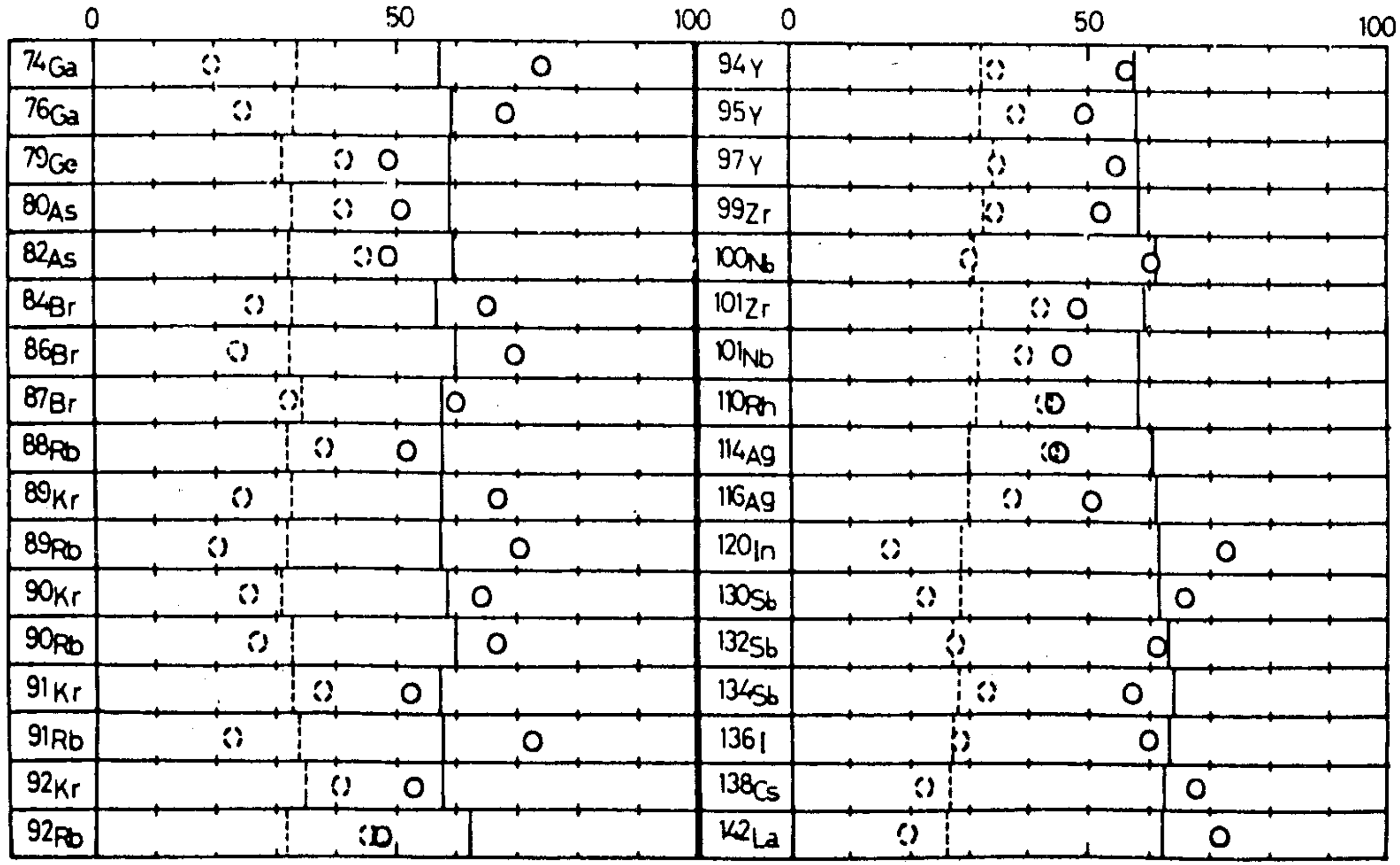


Fig. 8 **Percentage of average beta-particle and gamma-ray energies from fission products, $Q_{00}$ fixed to 1.0 MeV. Here, a dot = beta energy, a solid = beta-particle plus gamma-ray energy, a circle = experimental value (Refs. 4 and 2), and a line = calculated value. (Total decay energy = 100%.)**

Fig.9 Calculated beta- and gamma-ray energies released from short-lived FPs. Also shown in circles, triangles, and stars, are library values.

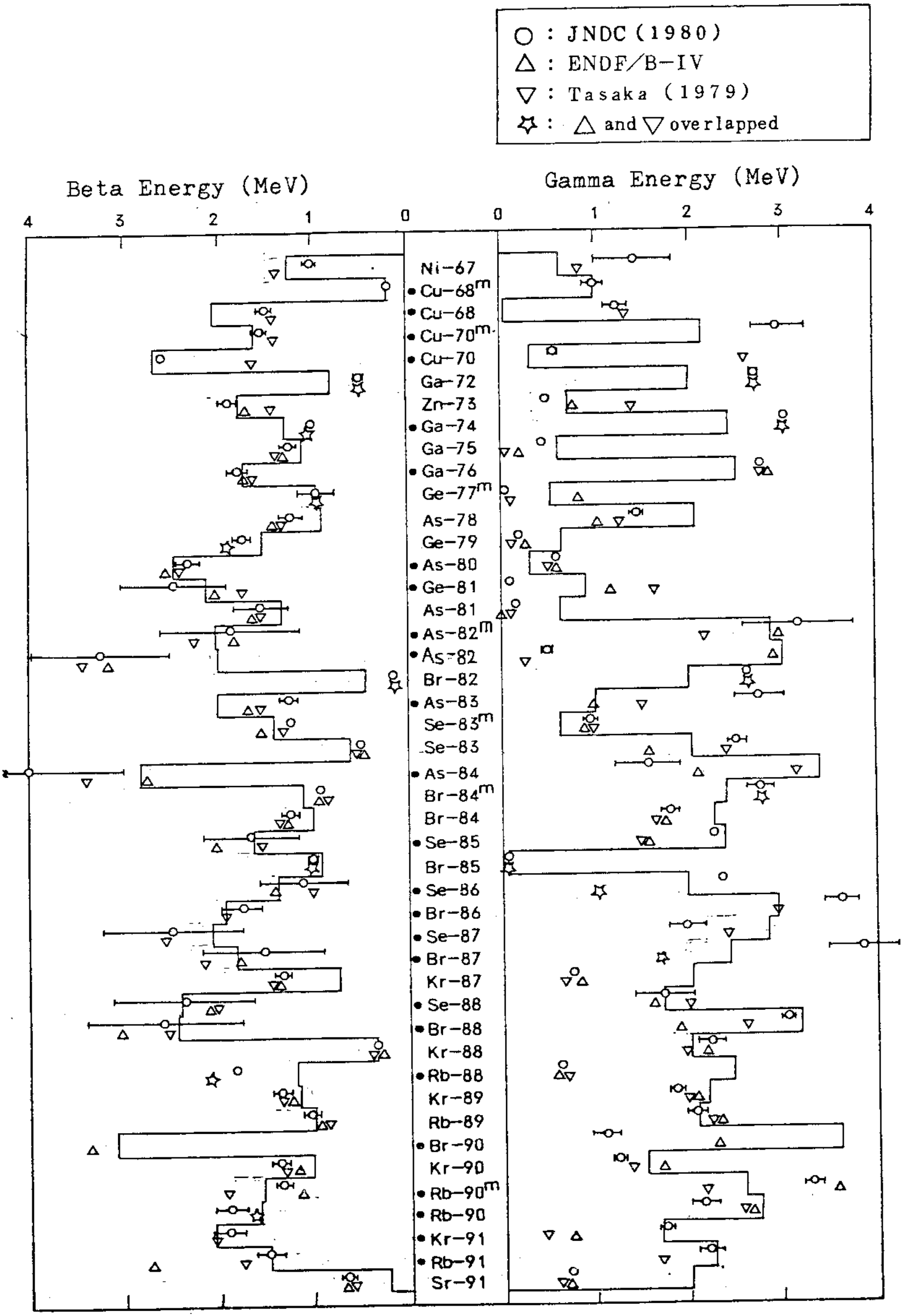

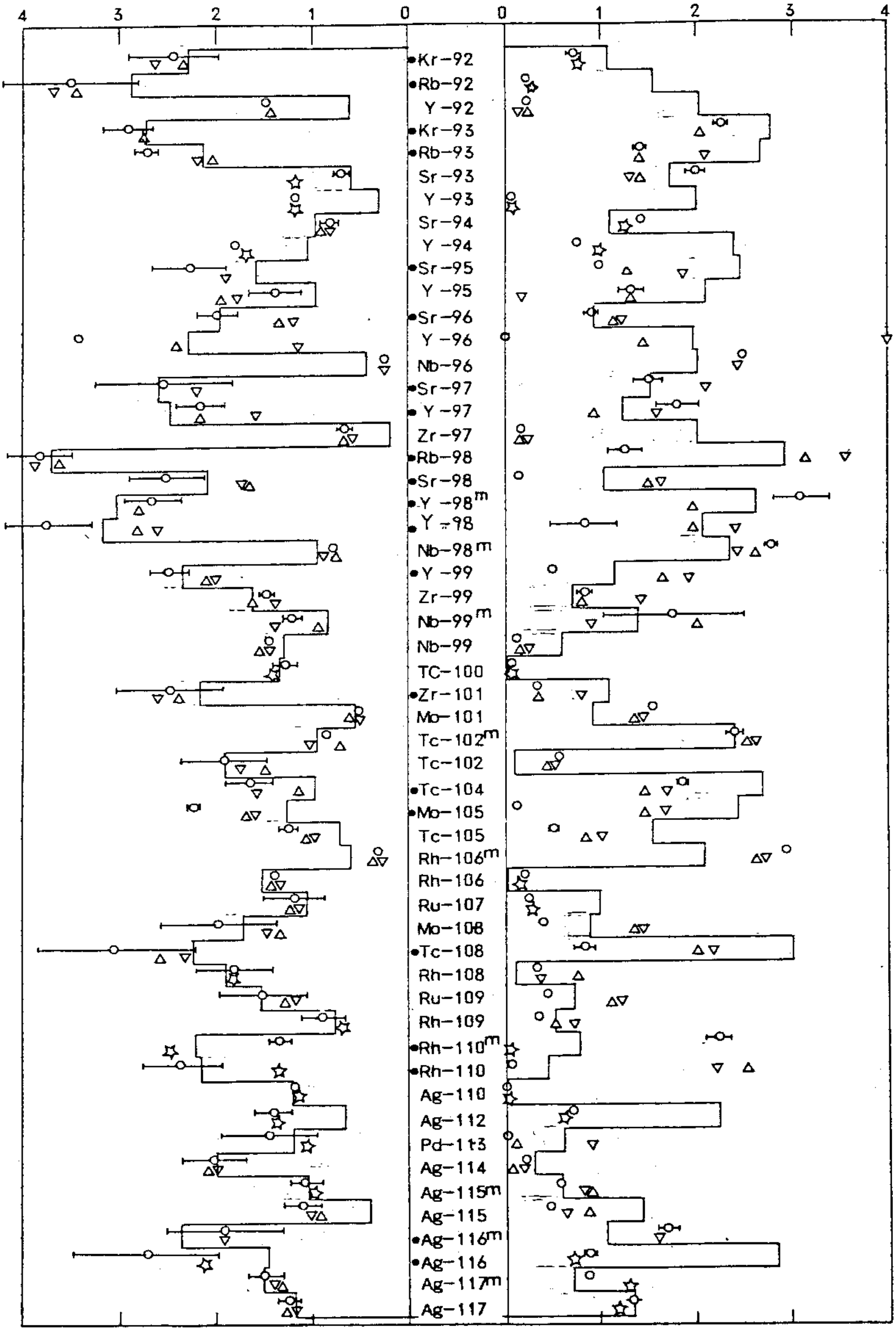
4
3
2
1
0
0
1
2
3
4
Kr－92
Rb－92
Y－92
Kr－93
Rb－93
Sr－93
Y－93
Sr－94
Y－94
Sr－95
Y－95
Sr－96
Y－96
Nb－96
Sr－97
Y－97
Zr－97
Rb－98
Sr－98
Y－98m
Y－98
Nb－98m
Y－99
Zr－99
Nb－99m
Nb－99
Tc－100
Zr－101
Mo－101
Tc－102m
Tc－102
Tc－104
Mo－105
Tc－105
Rh－106m
Rh－106
Ru－107
Mo－108
Tc－108
Rh－108
Ru－109
Rh－109
Rh－110m
Rh－110
Ag－110
Ag－112
Pd－113
Ag－114
Ag－115m
Ag－115
Ag－116m
Ag－116
Ag－117m
Ag－117

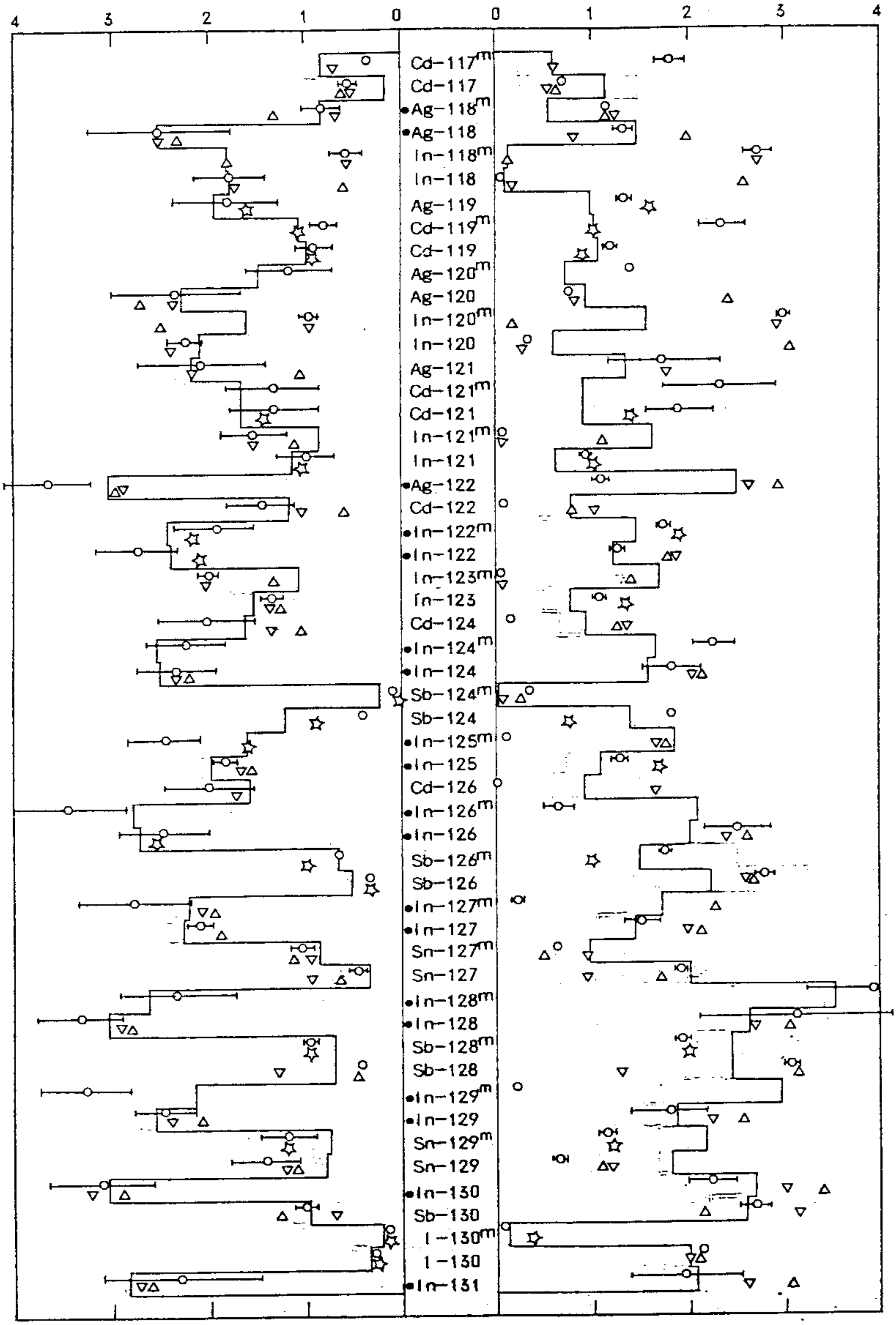
4
3
2
1
0
0
1
2
3
4
Cd-117m
Cd-117
•Ag-118m
•Ag-118
In-118m
In-118
Ag-119
Cd-119m
Cd-119
Ag-120m
Ag-120
In-120m
In-120
Ag-121
Cd-121m
Cd-121
In-121m
In-121
•Ag-122
Cd-122
•In-122m
•In-122
In-123m
In-123
Cd-124
•In-124m
•In-124
Sb-124m
Sb-124
•In-125m
•In-125
Cd-126
•In-126m
•In-126
Sb-126m
Sb-126
•In-127m
•In-127
Sn-127m
Sn-127
•In-128m
•In-128
Sb-128m
Sb-128
•In-129m
•In-129
Sn-129m
Sn-129
•In-130
Sb-130
I-130m
I-130
•In-131

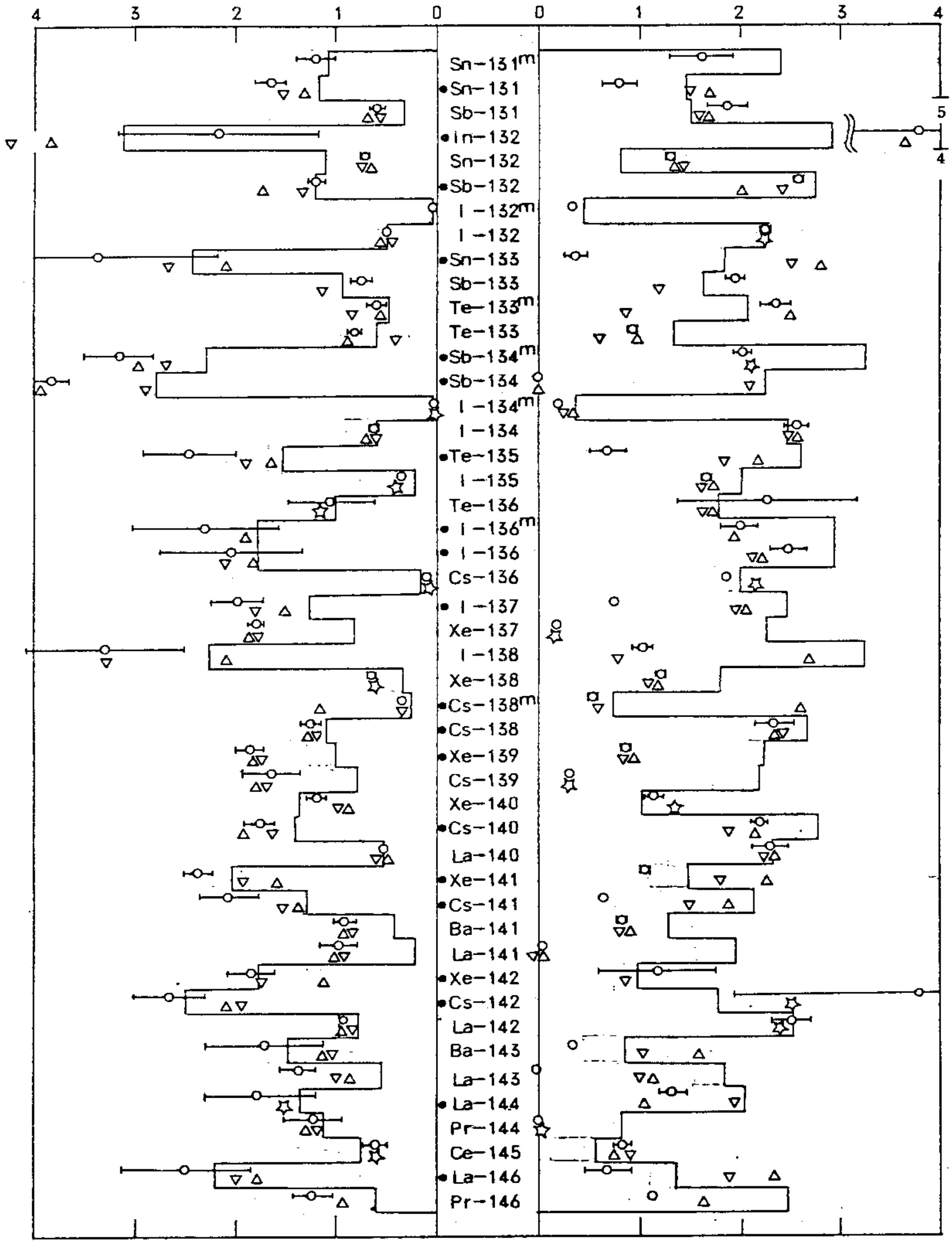
4
3
2
1
0
0
1
2
3
4
5
4
Sn-131m
•Sn-131
Sb-131
•In-132
Sn-132
•Sb-132
I-132m
I-132
•Sn-133
Sb-133
Te-133m
Te-133
•Sb-134m
•Sb-134
I-134m
I-134
•Te-135
I-135
Te-136
• I-136m
• I-136
Cs-136
• I-137
Xe-137
I-138
Xe-138
•Cs-138m
•Cs-138
•Xe-139
Cs-139
Xe-140
•Cs-140
La-140
•Xe-141
•Cs-141
Ba-141
La-141
•Xe-142
•Cs-142
La-142
Ba-143
La-143
• La-144
Pr-144
Ce-145
• La-146
Pr-146

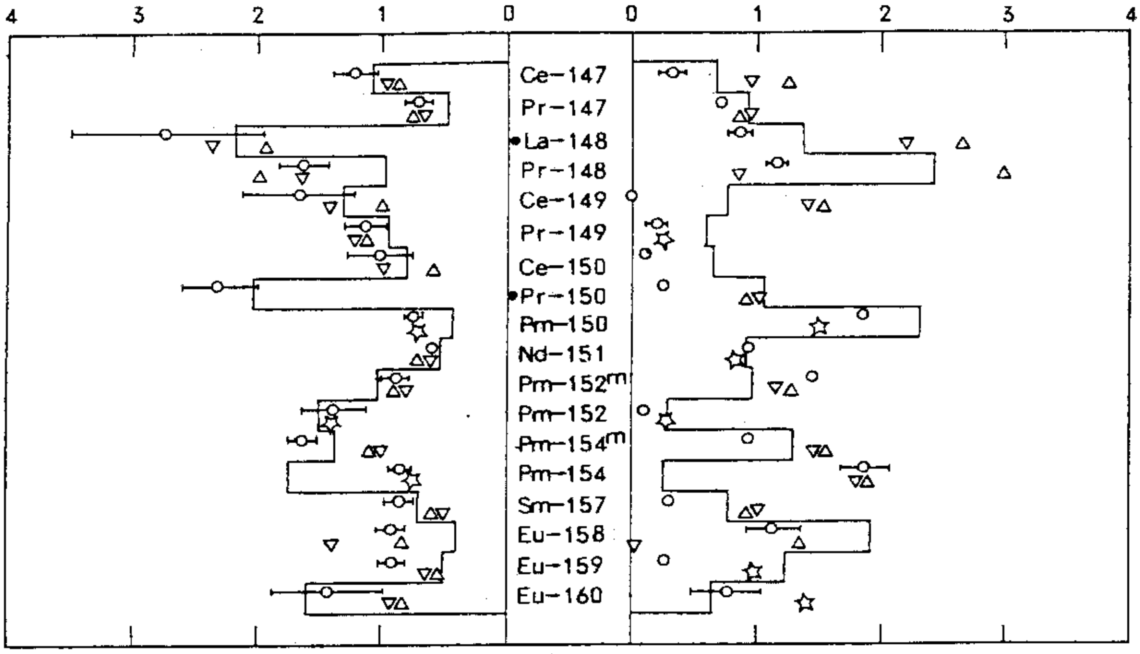
4
3
2
1
0
0
1
2
3
4
Ce−147
Pr−147
La−148
Pr−148
Ce−149
Pr−149
Ce−150
Pr−150
Pm−150
Nd−151
Pm−152m
Pm−152
Pm−154m
Pm−154
Sm−157
Eu−158
Eu−159
Eu−160

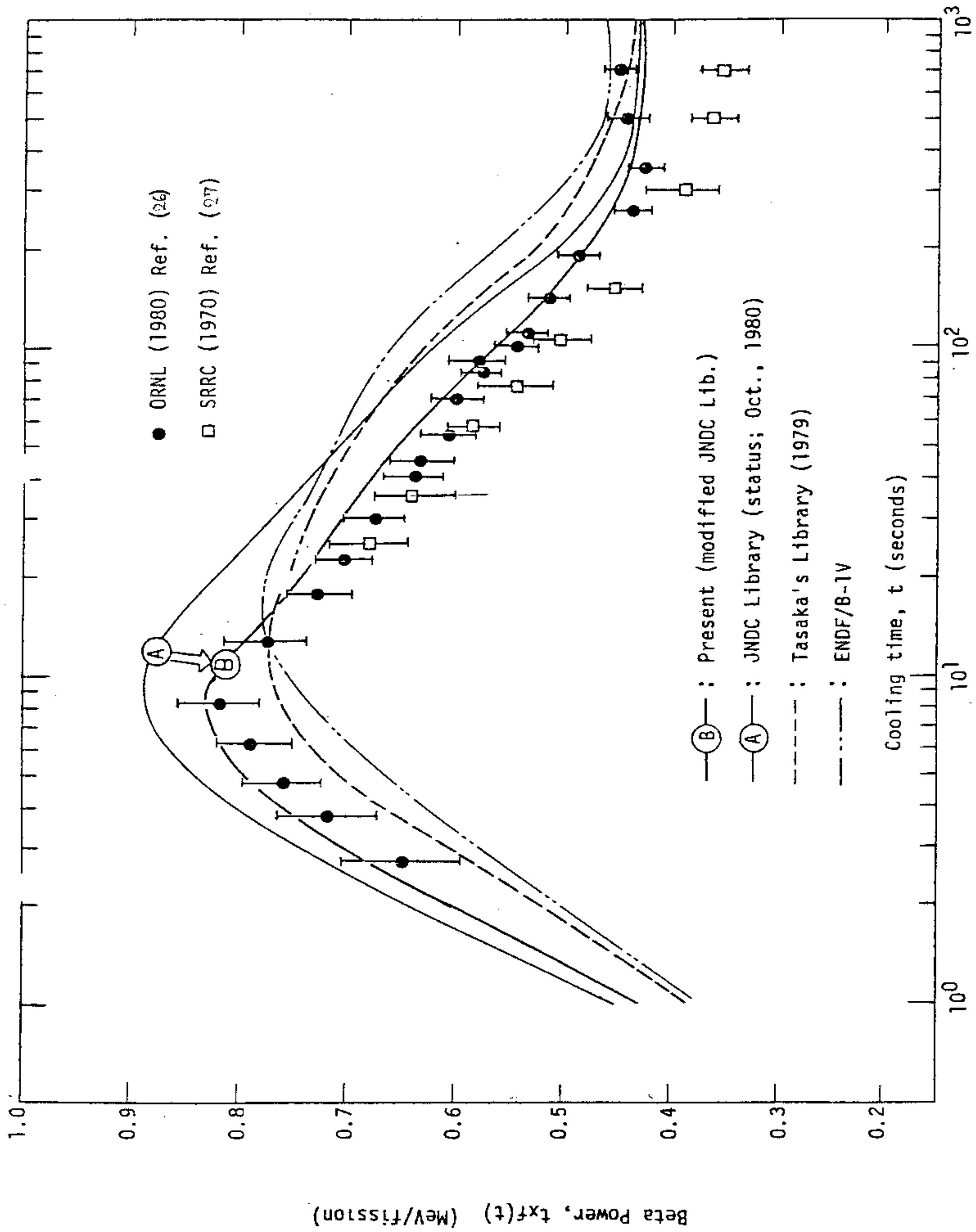


Fig.10 Effect of the introduction of theoretical values of $\overline{E}_\beta$ on U-235 beta-heating

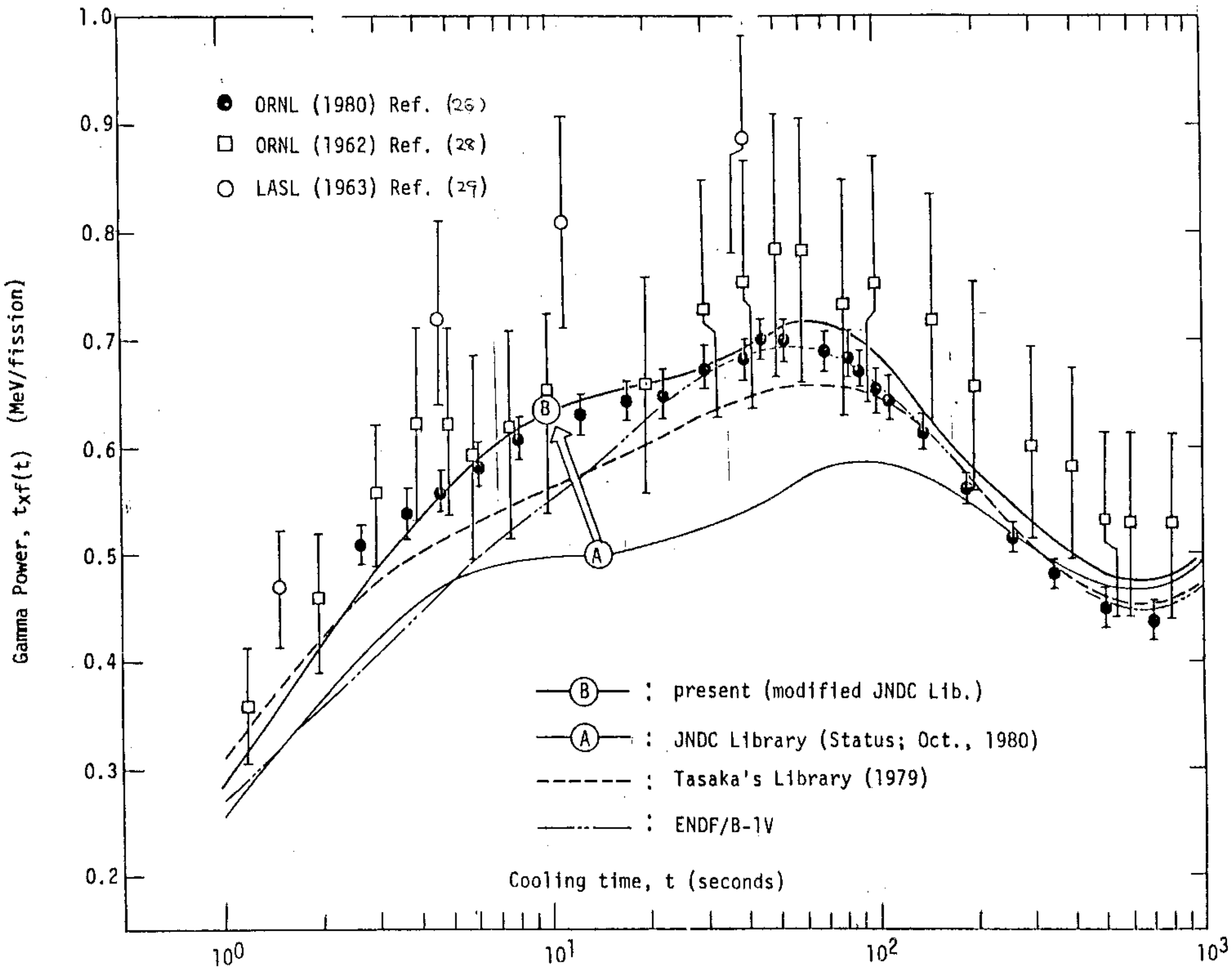


Fig.11 Effect of the introduction of theoretical values of $\overline{E}_{\gamma}$ on U-235 gamma-heating

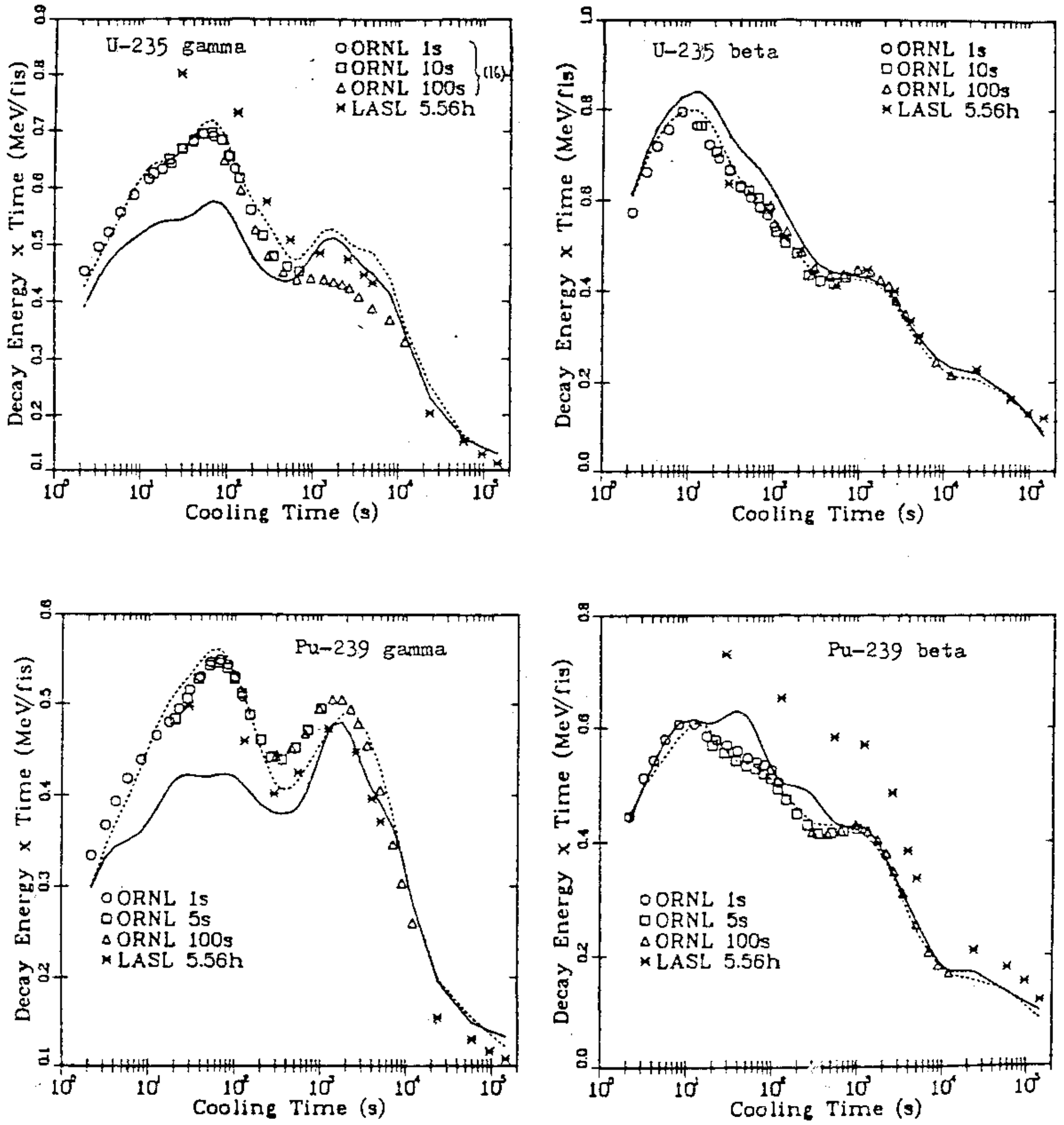


Fig.12 **Effect of the introduction of the theoretical values of $\overline{E}_\beta$ and $\overline{E}_\gamma$ on beta and gamma-decay heats based on ENDF/B-V data library (——— :original, ------- :after the introduction, calculated by T.R.England, Los Alamos Scientific Laboratory, et al.**
(See also reference 30).)

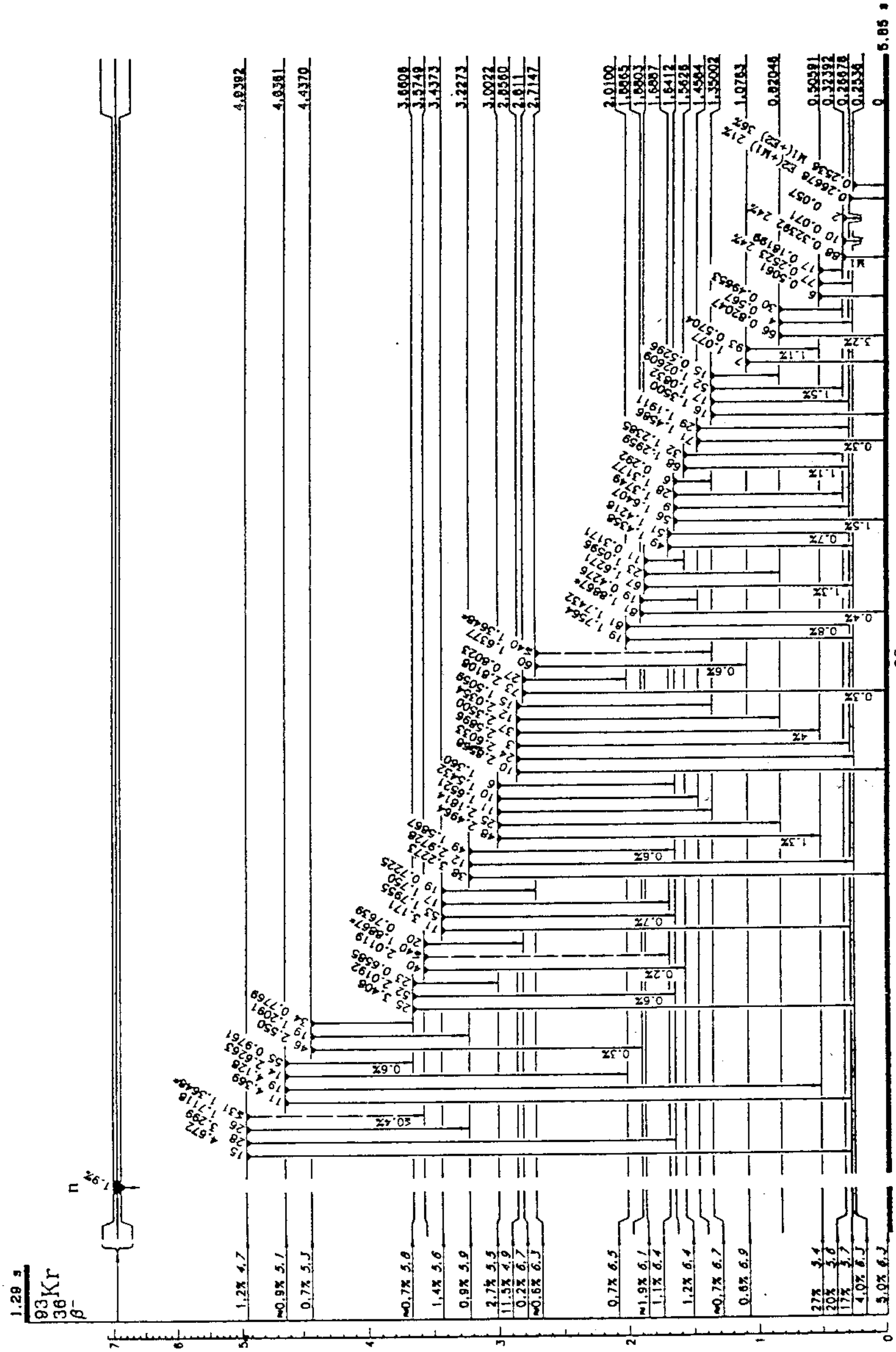


Fig.13 Decay scheme of Kr-93 (from Tables of Isotopes, 7th ed)

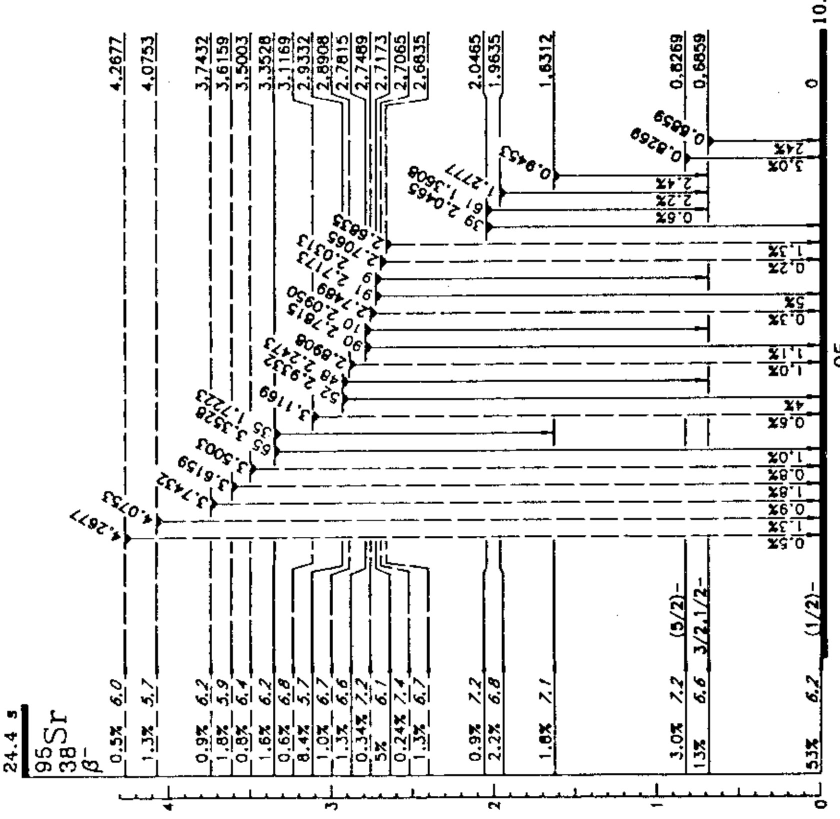

Fig. 14 Decay scheme of $^{95}Sr$ (from Tables of Isotopes, 7th ed.)

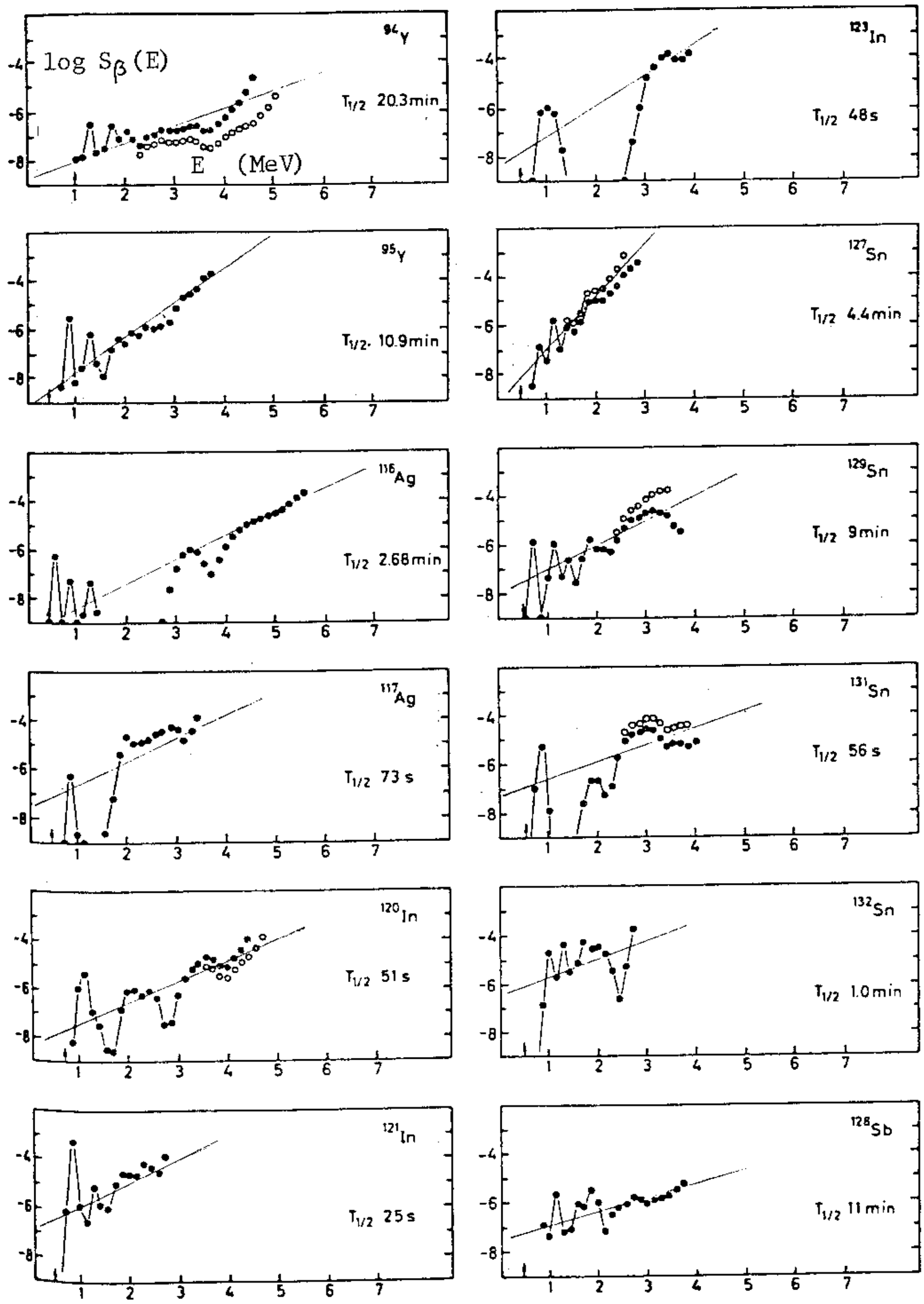


------ : rough linear fit by eye-guide

Fig.15 Examples of measured beta-strength functions (from K.H.Johansen, K.B.Nielsen, G.Rudstam, Nucl.Phys.,A203,481(1973))

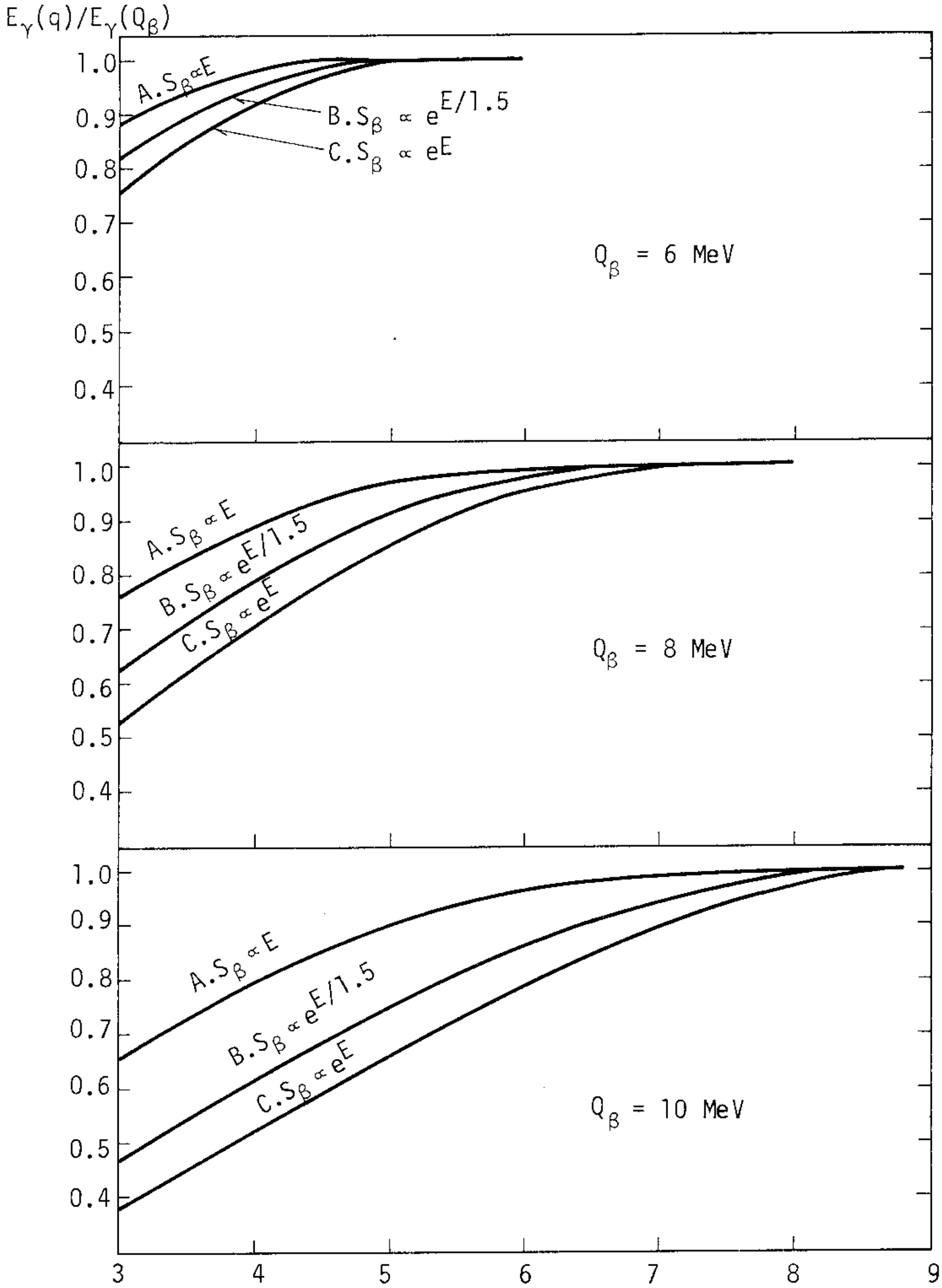


Fig. 16 Decrease of E due to possible missing of beta strengths at high excitation